BIOCHEMISTRY
including biophysical chemistry & molecular biology

Article

pubs.acs.org/biochemistry

Processive Degradation of Unstructured Protein by *Escherichia coli* Lon Occurs via the Slow, Sequential Delivery of Multiple Scissile Sites Followed by Rapid and Synchronized Peptide Bond Cleavage Events

Natalie Mikita, Iteen Cheng, Jennifer Fishovitz, Jonathan Huang, and Irene Lee*

Department of Chemistry, Case Western Reserve University, Cleveland, Ohio 44106, United States

Supporting Information

ABSTRACT: Processive protein degradation is a common feature found in ATP-dependent proteases. This study utilized a physiological substrate of *Escherichia coli* Lon protease known as the lambda N protein (λN) to initiate the first kinetic analysis of the proteolytic mechanism of this enzyme. To this end, experiments were designed to determine the timing of three selected scissile sites in λN approaching the proteolytic site of ELon and their subsequent cleavages to gain insight into the mechanism by which ATP-dependent proteases attain processivity in protein degradation. The kinetic profile of peptide bond cleavage at different regions of λN was first detected by the iTRAQ/mass spectrometry technique. Fluorogenic λN constructs were then generated as reporter substrates for transient kinetic characterization of the ATP- versus AMPPNP-dependent peptide bond cleavage and the delivery of the scissile sites near the amino- versus carboxyl-terminal of the λN protein to the proteolytic site of ELon. Collectively, our results support a mechanism by which the cleavage of multiple peptide bonds awaits the "almost complete" delivery of all the scissile sites in λN to the proteolytic site in an ATP-dependent manner. Comparing the time courses of delivery to the active site of the selected scissile sites further implicates the existence of a preferred directionality in the final stage of substrate delivery, which begins at the carboxyl-terminal. The subsequent cleavage of the scissile sites in λN, however, appears to lack a specific directionality and occurs at a much faster rate than the substrate delivery step.

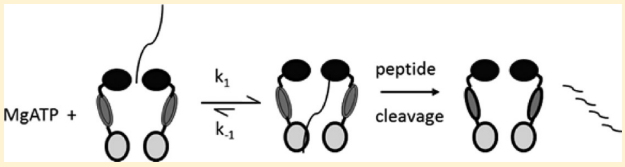

Lon, also known as protease La, is an ATP-dependent protease functioning to degrade certain damaged proteins and short-lived regulatory proteins in the cell.[1−7] This enzyme possesses intrinsic ATPase activity that is enhanced during protein or peptide degradation; however, the two processes are not stoichiometrically linked.[8] As a homo-oligomer, Lon is composed of an ATPase and a protease domain in each enzyme subunit.[9,10] Oligomerization requires Mg^{2+} but not ATP.[9] Analytical ultracentrifugation and electron microscopy studies reveal that bacterial Lon proteases are hexameric ring-shaped structures containing a central cavity, where the proteolytic sites reside.[9,10] Limited proteolytic footprinting studies of ELon reveals that adenine nucleotide protects the enzyme from nonspecific proteolysis, thereby indicating the existence of at least one conformational change generated by binding to ATP.[11,12] The presence of a proteolytic dyad consisting of a conserved Ser and Lys has been implicated.[13] Within the full-length Lon protein, mutation of either Ser or Lys to Ala in the catalytic dyad abolishes proteolytic but not ATPase activity.[13−16] By contrast, mutation of the ATP-binding site abolishes both the ATPase and proteolytic activities of Lon.[17] Therefore, despite the presence of a proteolytic dyad, the proteolytic activity of Lon is affected by the binding and hydrolysis of ATP.

Based upon the general mechanism of ATP-dependent proteolysis, it is proposed that Lon, like other proteases in the family, coordinates repeated cycles of ATPase and peptidase activity to completely degrade a protein substrate containing multiple sites, without generating partially digested substrate intermediates. This is referred to as processive degradation in the field.[18−20] It is suggested that the unfolding and vectorial delivery of substrate to the proteolytic site constitutes the rate-limiting step, and is dependent on the ATPase activity.[21] The binding and hydrolysis of ATP induces a series of conformational changes within the enzyme subunits that leads to unfolding of substrate, followed by internalization (also known as translocation) of the protein substrate into the central cavity.[22,23] Both unfolding and translocation are hypothesized to be carried out by repetitive cycles of ATP hydrolysis, and delivery into the central cavity is thought to happen via a threading mechanism[18,24] (i.e., the polypeptide substrate is transported through the narrow central pore of the enzyme in a roughly linear conformation). The unfolded and translocated polypeptide substrates are sequestered within the central cavity of the protease machinery (the proteolytic chamber), where peptide bond cleavage occurs.[21] Since the degradation of protein substrates only generates completely digested peptides ranging from 5 to 20 amino acids without generating partially digested protein intermediates, it is concluded that ATP-dependent proteases degrade their substrates processively.[25,26] However, it is not clear how the substrate translocation event is

Received: June 27, 2013
Published: July 3, 2013

   dx.doi.org/10.1021/bi4008319 | *Biochemistry* 2013, 52, 5629−5644

coordinated with peptide bond cleavage to completely digest substrates during the reaction time course.

Our current understanding of processivity in ATP-dependent proteolysis stems primarily from studies on the heterosubunit ATP-dependent proteases such as ClpXP or ClpAP.[18,20,27−31] These Clp protease complexes recognize unique peptide sequence tags, such as the SsrA tag, on a protein substrate to initiate substrate translocation.[32] Using model substrates containing the SsrA tag, it has been shown that the translocation of protein or polypeptide substrates by the ATPase subunit in ClpX or ClpP originates from the SsrA tag and exhibits processivity.[33] While these studies reveal the contribution of the ATPase activity in rendering processivity in substrate interaction, they do not explain how the ATPase and peptidase activities are coordinated to generate only completely digested peptides. As illustrated in Scheme 1, depending on the timing by which the different scissile sites in a protein substrate gain access to the proteolytic site and when peptide bond cleavage occurs, two different protein degradation mechanisms could be expected. In model 1, peptide bond cleavage occurs after complete substrate translocation to generate only fully digested peptide products. The delivery of different Lon cleavage sites in the substrate to the proteolytic chamber should occur before initiation of any peptide bond cleavage. In model 2, the cleavage of each scissile peptide bond is flanked by a substrate translocation event, while partially digested substrate remains bound to Lon during the reaction. In this case, a cycle of delivery/peptide cleavage event is anticipated to occur for each Lon cleavage site such that a specific set rate constant for the translocation and peptide bond cleavage will be detected for each cycle. The two models can be distinguished by detecting whether the peptide bonds in a protein substrate are cleaved with comparable (model 1) or different (model 2) kinetic parameters. In model 1, it is also anticipated that the rate constants for all the scissile sites entering the proteolytic chamber to be higher than the rate constant for peptide bond cleavage.

Scheme 1. Two Possible Models for λN Degradation by Lon[a]

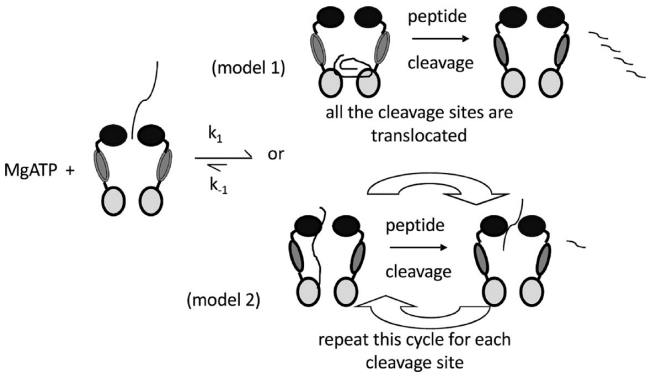

[a]Comparing the timing of the translocation and cleavage of the N-terminal versus the C-terminal site using pre-steady-state techniques will reveal a concerted (model 1) versus sequential (model 2) peptide bond cleavage mechanism.

The goal of this study is to determine the timing by which *Escherichia coli* Lon (ELon) catalyzes the ATP- and AMPPNP-dependent cleavage of λN near the amino versus carboxyl termini in order to obtain insights into how processive peptide bond cleavage occurs. The λN protein is a transcriptional regulatory protein functioning to enable RNA transcription beyond the transcription termination signal in *E. coli* cells during λ phage infection.[34,35] The timing of λN expression and degradation dictates whether λ phage adopts a lytic or a lysogenic life cycle in the infected host. When free in solution, λN does not adopt any defined structure.[35−38] *In vitro*, ELon degrades the purified λN protein in the presence of ATP or AMPPNP (a nonhydrolyzable analog of ATP).[25] Despite the differences in the rate of λN degradation exhibited by the two nucleotides (faster in the presence of ATP), the same hydrolyzed peptide products were generated upon complete degradation.[25] Due to a lack of defined structure and its physiological relevance as a Lon substrate, λN serves as an ideal substrate for using a systematic approach to study the processive protein degradation of ELon. Since the unfolding of this substrate is not necessary, we will only need to consider the delivery to the active site and cleavage of the multiple peptide bonds within the substrate during its degradation. Because λN contains only 107 amino acids and lacks a defined structure, chemically modified forms of this protein can be readily synthesized to produce a large quantity of the reagents for transient kinetic studies. Elucidating the kinetic mechanism of λN degradation will reveal the enzyme intermediates generated along the reaction pathway whose formations are facilitated by ATP binding and hydrolysis, which are also responsible for mediating processive peptide bond cleavage.

MATERIALS AND METHODS

Materials. Restriction endonucleases were purchased from Promega or New England Biolabs. Oligonucleotides were custom-synthesized by IDT, Inc. Solvents, buffers, chromatography resin, antibiotics, culture media, and PEI cellulose TLC plates were purchased from Fisher Biotechnology or Sigma/Aldrich. Plasmids used for protein expression and competent cells were purchased from Invitrogen and Novagen. [α^{32}P]ATP was purchased from Perkin-Elmer Life Science. FRλN001 and λNΔ1−34 were synthesized by GenScript, and FRλN006 was synthesized by LifeTein.

General Methods. ELon purification procedures were performed as described elsewhere.[39] All enzyme concentrations were reported as ELon monomer concentrations. Experiments were performed at least in triplicate. In all cases, comparable results were obtained. Either representative data or averaged data were shown.

Generation of λN Variants. For the construction of λN001, λN002, and λN006, the DNA encoding for the respective gene was synthesized by Genescript in the pUC57 plasmid, with a cysteine inserted at position 26 for λN001, position 42 for λN002, and position 99 for λN006. The endogenous Cys in WT λN was replaced with a Leu and all endogenous Trp were replaced with Phe. The respective gene cassette was subcloned into the pCOLA-Duet vector using the *Bam*HI and *Hin*dIII restriction sites. The resulting λN constructs were expressed with an N-terminal 6x His tag in BL21 (DE3) *E. coli*, which lacks endogenous Lon protease. N-his-λN (N-terminal his-tagged λN), C-his-λN (C-terminal his-tagged λN), N-his-λNΔ99−107, λN001, λN002, and λN006 were expressed in BL21 (DE3) and purified as described previously.[40] The protein was quantified using the Bradford assay.[41]

Preparation of Dansylated λN Variants. The purified λN001, λN002, and λN006 were labeled with dansyl aziridine

dx.doi.org/10.1021/bi4008319 | *Biochemistry* 2013, 52, 5629−5644

(Invitrogen). Dansyl aziridine was prepared in dimethylsulfoxide and was added to the λN protein in 5-fold excess. The reaction was gently agitated at room temperature overnight and then quenched with β-mercaptoethanol. Unreacted dye was removed by dialyzing λN into storage buffer containing 20 mM Tris, 50 mM NaCl, 1 mM β-mercaptoethanol, and 20% glyercol. The labeled protein was then quantified using the Bradford assay.[41] The extent of dansyl labeling in each protein was determined by the absorbance of dansyl at A_{340} and compared to the concentration of protein.

Characterization of the Degradation of Full Length versus Truncated λN by SDS-PAGE. To compare the ATP-dependent degradation profiles of WT versus truncated λN, 10 μM of protein substrate (N-his-λN, Δ1−34λN, or N-his-λNΔ99−107) was incubated with 5 mM ATP and 1 μM WT ELon at 37 °C in a reaction buffer containing 50 mM Tris-HCl (pH 8.1), 15 mM $Mg(OAc)_2$, and 5 mM DTT. At 0, 5, and 10 min, reaction aliquots were quenched with 5x SDS-PAGE loading dye. All quenched reaction time points were resolved on a 12.5% SDS-PAGE gel and stained with Coomassie Brilliant Blue to detect the undigested substrates.

Measuring N-his-λNΔ99−107 Binding Using Radiolabeled ATPase Assay. N-His-λNΔ99−107 protein binding to WT ELon was detected by ATP hydrolysis at 37 °C by radiolabeled ATPase assay as described previously and all reactions were performed at least in triplicate.[42] Briefly, each reaction mixture contained 50 mM Tris-HCl (pH 8.1), 5 mM $Mg(OAc)_2$, 2 mM DTT, 500 μM ATP, and varied λNΔ99−107 concentrations from 1 μM to 25 μM. Reactions were initiated by 100 nM WT ELon monomer and incubated at 37 °C. Subsequently, 5 μL aliquots were quenched at various time points from 0 to 8 min in 10 μL of 0.5 N formic acid. A 3 μL aliquot of the reaction was spotted directly onto a PEI cellulose TLC plate (10 cm × 20 cm) and developed in 0.3 M potassium phosphate buffer (pH 3.4). Radiolabeled ADP nucleotide was then quantified using the Packard Cyclone storage phosphor screen Phosphor imager purchased from Perkin-Elmer Life Science. To compensate for slight variations in spotting volume, we corrected the concentration of ADP product obtained at each time point using an internal reference as shown in eq 1

$$[\mathrm{ADP}] = \left(\frac{\mathrm{ADP_{dlu}}}{\mathrm{ATP_{dlu}} + \mathrm{ADP_{dlu}}}\right)[\mathrm{ADP}] \quad (1)$$

The rates of the reactions for ADP production were converted to $k_{obs,\lambda N\Delta 99-107}$ values by dividing the steady-state rates with enzyme concentration. The $k_{obs,\lambda N\Delta 99-107}$ values were fit to eq 2 where $k_{obs,\lambda N\Delta 99-107}$ is the observed rate constant, $k_{obs,max}$ is the maximal rate, B is the N-his-λNΔ99−107 concentration, and $K_{d,\lambda N\Delta 99-107}$ is the binding constant for N-his-λNΔ99−107 constant and M is the start point.

$$k_{obs,\lambda N\Delta 99-107} = \frac{k_{obs,max}[B]}{K_{d,\lambda N\Delta 99-107} + [B]} + M \quad (2)$$

Characterization of the ATP- and AMPPNP-Dependent Degradation of N-his-λN. λN degradation assays contained 50 mM HEPES (pH 8), 75 mM KOAc, 15 mM $Mg(OAc)_2$, 5 mM DTT, 65 μM N-his-λN, and 5 mM nucleotide and the reaction was initiated with 6 μM WT ELon at 37 °C. At 0, 5, 10, and 20 min, reactions with N-his-λN and ATP or AMPPNP were quenched with 5x SDS-PAGE loading dye and incubated at 100 °C for 1 min. N-his-λN aliquots were then run on a 12.5% SDS-PAGE gel and then stained and destained with Coomassie Brilliant Blue to detect the undigested substrates.

Western Blot Analysis of λN Degradation. λN degradation assays were run as above with either 65 μM N-his-λN or C-hisλN and 5 mM AMPPNP. At 0 and 30 min, reaction aliquots were quenched with 5x SDS-PAGE loading dye and incubated at 100 °C for 1 min. The aliquots were loaded and run on a 17% SDS-PAGE gel for Western blotting. The proteins were transferred to a nitrocellulose membrane and blocked with TBST (Tris-buffered saline [pH 7.6], 0.1% Tween-20) with 1% bovine serium albumin overnight at 4 °C. The nitrocellulose was incubated with anti-His (1:500; Invitrogen, Life Technologies, Camarillo, CA, USA) for 1 h. After extensive washing with TBST, the membrane was incubated for 1 h in goat antimouse IgG alkaline phosphatase secondary antibody (1:3000, Sigma-Aldrich, St. Louis, MO, USA). Protein bands were visualized using BCIP/NBT.

Quantification of the Time Courses of ATP-Dependent Degradation of Unlabeled λN by ELon Using Isobaric Tag for Relative and Absolute Quantization (iTRAQ)/Mass Spectrometry Analysis. Ten micromolar of monomeric WT ELon (final concentration) was mixed with 50 μM N-his-λN and 1 mM ATP (final concentration) in a chemical quench flow instrument (KinTek) in a reaction buffer containing 50 mM HEPES, pH 8; 2 mM $Mg(OAc)_2$, 2 mM TCEP; 0.05% Tween 20. Reaction time points at 1, 3, 5, 10, 20, 30, and 60 s were obtained by quenching a reaction aliquot with 0.5 N formic acid. For the 0 time point, reaction aliquot omitting ELon was quenched with 0.5 N formic acid. The quenched reaction time points were frozen at −80 °C and submitted to the Center for Advanced Proteomics Research at the University of Medicine and Dentistry at New Jersey, NJ, USA for 8-plex iTRAQ analysis. In brief, the amino groups of the ELon-digested λN peptide products (from eight time points) were labeled by the respective iTRAQ tag and then desalted. The desalted time points were subjected to 2D liquid chromatography (cation exchange and C18 reverse phase) and then analyzed on a orbitrap mass spectrometer. Duplicate assays were performed. Peptides were identified from the degradation profile of λN by ELon and some sequences were further confirmed by manual evaluation of the MS/MS spectra performed by Dr. Tong Liu at UMDNJ. The standardized time courses for the generation of different hydrolyzed peptide products were obtained by plotting the ratio of the m/z intensity of the respective peptide at the indicated time point over the 60 s time point, versus the corresponding time of digestion. The raw data of the 8-plex iTRAQ data are supplied in Supporting Information (S3).

Monitoring the ATP-Dependent Degradation of Fluorescently Labeled λN (FRλN) by Steady State Kinetics. The cleavage of fluorescently labeled sites in λN were measured using a Fluoromax 4 spectrofluorimeter (Horiba Group) as described previously.[39] Reactions contained 50 mM HEPES pH 8.0, 5 mM $Mg(OAc)_2$, 2 mM DTT, 0.5, 1, 5, 10. 20, and 30 μM FRλN001 or FRλN006 (excitation at 320 nm and emission at 420 nm), and 150 nM WT ELon; the reaction was incubated for 1 min at 37 °C before being initiated by 1 mM ATP. All assays were performed at least in triplicate, and the averaged value of the rates determined for each substrate was fit to eq 3.

dx.doi.org/10.1021/bi4008319 | Biochemistry 2013, 52, 5629−5644

$$k_{obs,\lambda N,ATP} = \frac{k_{cat,\lambda N,ATP}[S]}{K_m + [S]} \quad (3)$$

where $k_{obs\lambda N,ATP}$ is the observed rate, $k_{cat\lambda N,ATP}$ is the max rate constant of product formation at saturating substrate, K_m is the Michaelis−Menten constant, and [S] is the substrate concentration.

Monitoring the Pre-Steady-State ATP and AMPPNP-Dependent Degradation of Fluorescently Labeled λN (FRλN) by Stopped Flow Kinetics. Pre-steady-state experiments were performed on a KinTek Stopped Flow controlled by the data collection software Stop Flow version 7.50 β. The sample syringes were maintained at 37 °C by a circulating water bath. In AMPPNP-dependent degradations, syringe A contained 10 μM WT ELon, 10 μM λN001A (10% FRλN001 and 90% λN001), or 10 μM λN006A (10% FRλN006 and 90% λN006), and reaction buffer (5 mM $Mg(OAc)_2$, 50 mM Tris-HCl (pH 8.1), 5 mM DTT, 30 mM KOAc, and 30 mM KPi). Syringe B contained 10 μM λN001 or 10 μM λN006, reaction buffer, and 2 mM AMPPNP. For all other reactions, syringe A contained 10 μM WT ELon, 8 μM λN001A, or 8 μM λN006A, and reaction buffer. Syringe B contained 8 μM λN001 or 8 μM λN006, reaction buffer, and 2 mM ATP, ADP, or no nucleotide. Protein cleavage was detected by an increase in fluorescence (excitation of 320 nm and emission with a 400 nm long-pass filter) following rapid mixing of the syringe contents in the sample cell over 200 s for AMPPNP, and 10 s for all others. The baseline of the fluorescence was normalized to zero, and the data shown are the results of averaging at least four traces. The concentration of the hydrolyzed peptide was calibrated by determining the maximum fluorescence generated per micromolar peptide due to complete digestion by trypsin under identical conditions on the stopped-flow. The lag equation was fit to the averaged time courses:

$$F = \nu_f t - \frac{\nu_f}{k_{lag}\{1 - \exp(-k_{lag}t)\}} \quad (4)$$

where F is the relative fluorescence intensity, v_f is the final velocity, t is the time in seconds, and k_{lag} is the apparent lag rate of the time courses.

Pseudo First Order Delivery of DansylλN to the Protoelytic Active Site in S679W ELon by Fluorescent Stopped Flow. Experiments to monitor the translocation of DansylλN with ELon (S679W and S679A) were performed on a KinTek Stopped Flow controlled by the data collection software Stop Flow version 7.50 β with a 0.5 cm path length. The sample syringes were maintained at 37 °C by a circulating water bath. Syringe A contained 10 μM S679A or S679W ELon monomer with 10 μM dansylλN (dansylλN001, dansylλN002, or dansylλN006) and reaction buffer (5 mM HEPES pH 8.0, 75 mM KOAc, 75 mM KPi, 5 mM $Mg(OAc)_2$, and 5 mM DTT). Syringe B contained 1 mM ATP or AMPPNP, 10 μM dansylλN, and reaction buffer. DansylλN translocating to S679A or S679W ELon was monitored by an increase in fluorescence (excitation 295 nm, emission 450 nm long-pass filter) upon rapid mixing of the syringe contents over 80 s for AMPPNP, 20 s for all others. In addition to monitoring excitation with 295 nm and emission with 450 nm long-pass filter, experiments were performed with excitation 295 nm and emission with a 340 nm band-pass filter monitor to view the changes in Trp fluorescence. The data shown are a result of averaging at least four traces. Each reaction was performed in triplicate. It should be noted that the PMT (photomultiplier tube) sensitivity was automatically adjusted by the instrument to optimize signal-to-noise. As a result, the relative amplitudes of the time courses do not reflect the stoichiometries of the enzyme intermediates monitored by the signals. The first-order rate constants of the reactions do not change because the dansyl absorbance in each reaction remains constant. The first 0.5 s of the average time courses of S679W ELon with ATP and dansylλN were fitted with eq 5 describing a single exponential

$$F = A_1 \exp(-k_{1,FRET,ATP}t) + C \quad (5)$$

where F is relative fluorescence, A_1 is the amplitude in relative fluorescence units, t is time in seconds, C is the end point, and $k_{1,FRET,ATP}$ is the first order rate constant associated with protein initiation. The averaged time courses of S679W ELon with AMPPNP and dansylλN were fitted with eq 6 describing a double exponential

$$F = A_1 \exp(-k_{1,FRET,AMPPNP}) + A_2(-k_{2,FRET,AMPPNP}) + C \quad (6)$$

where F is relative fluorescence, A_1 and A_2 are amplitudes in relative fluorescence units, t is time in seconds, C is the end point, k_1 is the first-order rate constant associated with the first phase of the reaction in per seconds, and k_2 is the first-order rate constant associated with the second phase of the reaction in per seconds.

Chemical-Quench ATPase Activity Assays. The pre-steady-state time courses for ATP hydrolysis were measured using a rapid chemical-quench-flow instrument from KinTek Corporation. The instrument was maintained at 37 °C by a circulating water bath. Syringe A contained 5 μM Lon (WT), with 8 μM λN substrate (λN001 or λN006), 5 mM $Mg(OAc)_2$, 50 mM HEPES (pH 8.1), 5 mM DTT, 75 mM KOAc, and 75 mM KPi. Syringe B contained 8 μM λN substrate (λN001 or λN006), 5 mM $Mg(OAc)_2$, 50 mM HEPES (pH 8.1), 5 mM DTT, 75 mM KOAc, 75 mM KPi, and 200 μM ATP containing 0.01% of [α-^{32}P]ATP at times (0−1.8 s) before quenching with 0.5 N formic acid and then extracting with 200 μL of phenol/chloroform/isoamyl alcohol at pH 6.7 (25:24:1). A 3 μL aliquot of the aqueous solution was spotted directly onto a PEI-cellulose TLC plate (10 × 20 cm), and the plates were developed in 0.75 M potassium phosphate buffer (pH 3.4) to separate ADP from ATP. The relative amount of radiolabeled ADP and ATP at each time point was quantified by a Cyclone Phosphor imager (Perkin-Elmer Life Science). To compensate for the slight variations in spotting volume, the concentration of the ADP product obtained at each time point was corrected for using an internal reference as shown in eq 1. All assays were performed at least in triplicate, and the average of those traces was used for data analysis. The burst amplitude and the burst rates were determined by fitting the k_{obs} data from 0 to 400 ms with eq 7

$$Y = A \exp^{-k_{burst}t} + C \quad (7)$$

where t is time in seconds, Y is [ADP] in micromolar, A is the burst amplitude in micromolar, k_{burst} is the burst rate constant in per seconds, and C is the end point. The observed steady-state rate constants ($k_{obs,ATP}$) were determined by fitting the data from 600 ms to 1.8 s with eq 8

$$Y = k_{obs,ATPase}X + k_{obs,ATPase}C \quad (8)$$

dx.doi.org/10.1021/bi4008319 | Biochemistry 2013, 52, 5629−5644

where X is time in seconds, Y is [ADP]/[E], $k_{obs,ATPase}$ is the observed steady-state rate constant in per seconds, and C is the y intercept. Data fitting was accomplished using the nonlinear regression program Kaleida-Graph (Synergy).

RESULTS

Degradation Profiles of N-his-λN. In an earlier study, truncated N-his-λN lacking residues 99−107 was shown to be degraded by ELon less efficiently than full length N-his-λN, suggesting that the C-terminal of λN plays a role in substrate degradation.[40] By contrast, the contribution of the N-terminal of λN is not known. As such, the degradation profiles of ATP-dependent degradation of N-his-λN, truncated N-his-λN lacking the C-terminal (N-his-λNΔ99−107), and truncated λN lacking the N-terminal and any his-tag (λNΔ1−34) were compared in this study. Figure 1A shows the degradation profiles of ELon degrading full-length N-his-λN, λNΔ1−34, and N-his-λNΔ99−107 in the presence of saturating [ATP] (5 mM) under identical conditions. Within 5 min into the reaction, full-length N-his-λN and λNΔ1−34 were mostly degraded, but N-his-λNΔ99−107 was still detected. According to Supporting Information S1 and S2, the time courses for the ATP-dependent degradation of full-length N-his-λN and C-his-λN are comparable, and λNΔ99−107 lacking a his-tag is still degraded less efficiently than full-length λN lacking a his-tag.

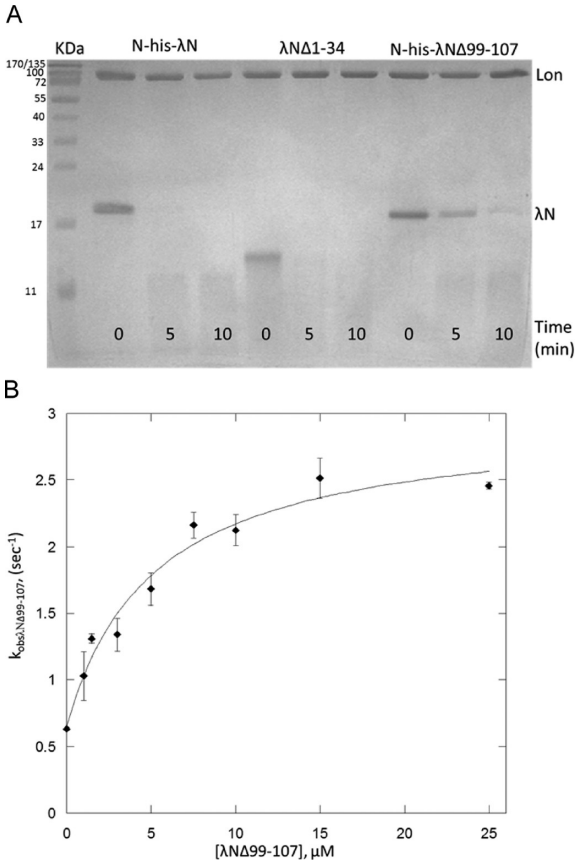

Figure 1. (A) Compare the time courses of λN deletion mutant degradations by WT ELon. Purified wild type N-his-λN and truncated λN lacking residues 1−34 (λNΔ1−34) or 99−107 (N-his-λNΔ99−107) were digested with ELon in the presence of 5 mM ATP and quenched at the times indicated. The progress of the degradation reactions was monitored by 12.5% SDS-PAGE as described in Materials and Methods. (B) Graphical representation of the stimulatory effect of N-his-λNΔ99−107 the ATPase activity of WT ELon. The k_{obs} values of ATP hydrolysis were determined at 500 μM ATP containing $\alpha[^{32}P]$ATP in the presence of 0, 1, 1.5, 3, 5, 7.5, 10, 15, and 25 μM N-his-λNΔ99−107 using the ATPase assay described in Materials and Methods. The data presented are the average of at least three independent assays. Error bars reflect values obtained from experimental deviations. Data was fit with eq 2 to yield $K_{d,λNΔ99-107}$ of 5.2 ± 1.7 μM.

Evaluate the Contribution of Residues 99−107 in the Degradation of λN. Since the C-terminal containing residues 99−107 contributes to the degradation efficiency of λN, this region likely interacts with ELon. To investigate this possibility, N-his-λNΔ99−107 was titrated against 100 nM ELon at saturating [ATP] to determine the concentration of N-his-λNΔ99−107 needed to attain 50% maximal ATPase stimulation. This assay was previously used to determine the K_d of N-his full length λN in ELon.[42] The ATPase activity was measured using a radioactive assay that quantified the amount of ADP generated over time using eq 1 shown in Methods and Materials. Dividing the observed rate of ATP hydrolysis by [monomeric Lon] yields the observed rate constant at the corresponding [N-his-λNΔ99−107]. As shown in Figure 1B, the $k_{obs,λNΔ99-107}$ values show a hyperbolic dependency against [N-his-λNΔ99−107], which upon fitting the data to eq 2 provides a $K_{d,λNΔ99-107}$ of 5.2 ± 1.7 μM. This value is ∼3.7-fold higher than the K_d of full-length N-his-λN (1.4 ± 0.6 μM), which was determined in an earlier publication.[42] Since the affinity as well as the degradation efficiency of the truncated substrate was reduced but not abolished, we conclude that residues in the deleted C-terminal of λN contribute to substrate degradation. However, additional recognition site(s) not found in either terminal of λN must be present to allow substrate recognition and degradation, albeit with reduced efficiency.

ATP- and AMPPNP-Dependent Degradation of His-Tagged λN. Previously, Maurizi showed that λN was degraded by ELon in the presence of the nonhydrolyzable ATP analog, AMPPNP, and the same peptide cleavage profile was detected in the ATP- versus AMPPNP-dependent degradation reaction.[25] Based on the peptide products generated, the possibility of ELon conducting nonprocessive as well as processive protein degradation was considered. Using a fluorogenic peptidase assay, we demonstrated that the k_{cat} of peptide bond cleavage was significantly reduced when ATP was substituted with AMPPNP.[43] Therefore, the ATP-versus AMPPNP-dependent degradation of λN may differ by the kinetics of substrate degradation. To evaluate this possibility, N-his-λN was degraded by ELon in the presence of 5 mM ATP versus AMPPNP, from which the reaction time courses were monitored by SDS-PAGE as shown in Figure 2A. Comparing the intensities of the intact substrate band of the ATP- versus AMPPNP-dependent reaction at the 5, 10, and 20 min time points reveals that the N-his-λN was degraded faster in the presence of ATP. Furthermore, a small amount of partially digested N-his-λN was detected at the 10- and 20-min time points in the AMPPNP-dependent but not ATP-dependent reaction, suggesting that in addition to reduced protein degradation kinetics, the lack of ATP hydrolysis allowed nonprocessive as well as processive protein degradation to occur.

dx.doi.org/10.1021/bi4008319 | Biochemistry 2013, 52, 5629−5644

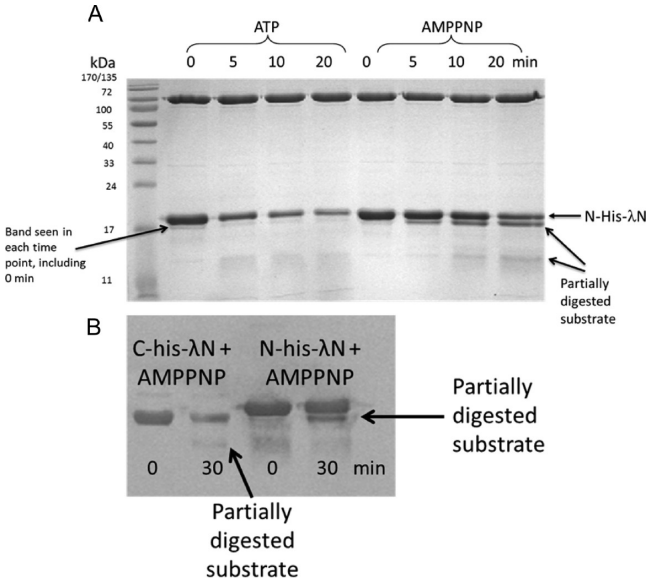

Figure 2. Degradation of λN by ELon in the presence of AMPPNP or ATP. Purified N-his-λN (65 μM) was digested by 6 μM ELon in the presence of 5 mM ATP or AMPPNP, and quenched at the times indicated. The degradations were monitored by 12.5% SDS-PAGE as described in Materials and Methods. Arrows point to degradation products only seen with AMPPNP. (B) Western blot of N-his-λN and C-his-λN degradation in the presence of AMPPNP with an antibody against a his-tag. N-his-λN protein (65 μM) was digested with 6 μM ELon and quenched at the time points indicated. Arrows point to degradation products.

To further determine if the partially digested N-his-λN was generated due to the presence of the his-tag, full-length λN containing a his-tag at the C-terminal (C-his-λN) was digested with ELon in the presence of 5 mM AMPPNP and subjected to Western blot analysis with anti-his-tag antibodies. Figure 2B reveals that partially digested λN was generated regardless of the location of a his-tag at the N- or C-terminal of λN, as an anti-his positive band corresponding to the mobility of a partially digested λN lacking an N-terminal but containing a C-terminal his-tag or vice versa is detectable. Compared to the degradation profiles of λN in the presence of ATP, the results presented in this section indicate that the catalytic efficiency as well as the extent of processivity of λN degradation is affected by the lack of ATP hydrolysis in the reaction, as AMPPNP is bound but not hydrolyzed by ELon. However, ATP hydrolysis is not required for the processive degradation of unstructured protein substrate. The fact that both his-tagged C- and N-termini were detected under identical time points indicates that no obligatory order of peptide bond cleavage occurred in the degradation of reactions.

Detecting the Kinetic Time Courses of WT ELon-Mediated Degradation of λN by iTRAQ Mass Spectrometry. To monitor the kinetics of N-his-λN degradation by WT ELon, a discontinuous chemical quench-flow mass spectrometry assay (RQ/MS) was used. In the RQ/MS assay, 5-fold the K_m level of N-his-λN was incubated with WT ELon at a saturating level of ATP (1 mM) and quenched at 0, 1, 3, 5, 10, 20, 30, and 60 s (see Supporting Information S3). These time points were chosen because no hydrolyzed peptide product was detected by LC/MS in the time points that were taken earlier than 1 s. The above reaction time points were quenched with 0.5 N formic acid to denature Lon and release digested λN products that were bound to Lon. The quenched time points were then derivatized with isobaric tagged succimides[44] such that the digested λN peptides in each time point were labeled with a specific m/z tag prior to analysis by LC/MS/MS. Peptides with identical sequences but tethered with different isobaric tags would have the same retention times on the LC traces. In the MS/MS spectra, the ratios of peptide quantities among different time points were deduced from the signal intensity ratios of the reporter groups in the isobaric tags, with m/z values of 113, 114, 115, 116, 117, 118, 119, and 121, respectively. The sequence of the digested peptide products was deduced and matched up with the published peptide sequences generated from the degradation of λN as summarized in S3. No partially digested λN sequence was detected. Of the peptides that were identified, the signal intensity of the reporter groups from each peptide was used to determine the ratio of the individual peptide at each time point. Analysis of the data done in duplicate showed approximately 40% of the digested λN peptides were identified and quantified. The time courses for the generation of three degraded λN peptides was used to illustrate the timing of peptide bond cleavage in the indicated regions in λN (Figure 3). Plotting the

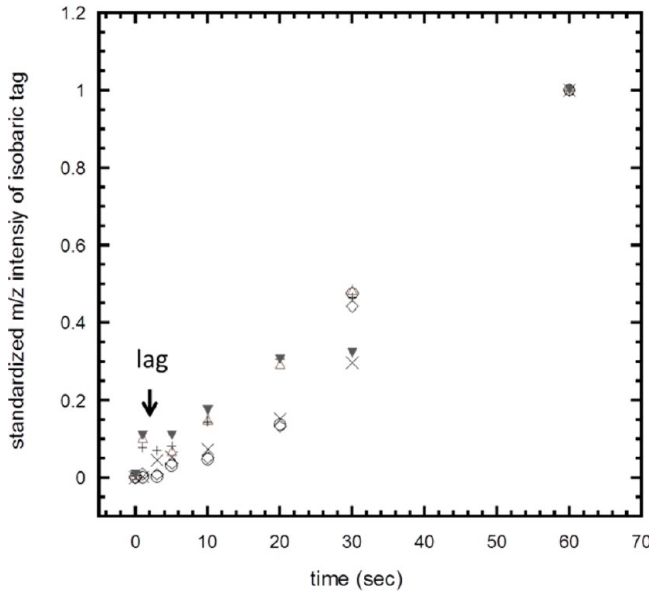

Figure 3. iTRAQ time courses for the ATP-dependent degradation of N-his-λN. The standardized m/z intensities of selected peptide fragments identified by two independent iTRAQ analyses (see Materials and Methods as well as Supporting Information S3) are plotted against their corresponding degradation time by WT ELon in the presence of saturating [ATP]. The standardized m/z intensity was obtained by dividing the observed intensity value at a given time by the intensity at 60 s, which was the longest degradation time of the analysis. The λN peptide fragments are: residues 31−40, trial 1 (○); residues 31−39 (◊), trial 1; residues 94−107, trial 1 (×); residues 31−40, trial 2 (+); residues 31−39, trial 2 (Δ); residues 94−107, trial 2 (▼).

relative m/z intensity of the respective isobaric labeled peptides against the corresponding reaction time points yielded the data shown in Figure 3. According to Figure 3, the time courses for the cleavage of the various scissile sites in λN are comparable. Furthermore, biphasic kinetic time courses were detected, with the first phase displaying slower reaction kinetics. As ELon was denatured prior to LC/MS analysis of the hydrolyzed peptide

dx.doi.org/10.1021/bi4008319 | Biochemistry 2013, 52, 5629−5644

A

FRλN001

^{1}M D A Q T R R R E R R A E K Q A Q F K A A N P L L Y(NO_2) V G V S **A K** P V N R P I L S **L N** K(Abz) R K P K S R V E S A L N P I D L T V L A E Y H K Q I E S N L Q R I E R K N Q R T F Y S K P G E R G I T **L S** G R Q K I K G K S I P L I

FRλN006

^{1}M D A Q T R R R E R R A E K Q A Q F K A A N P L L V G V S **A K** P V N R P I L S **L N** R K P K S R V E S A L N P I D L T V L A E Y H K Q I E S N L Q R I E R K N Q R T F Y S K P G E Y(NO_2) R G I T **L S** G R Q K(Abz) I K G K S I P L I

B

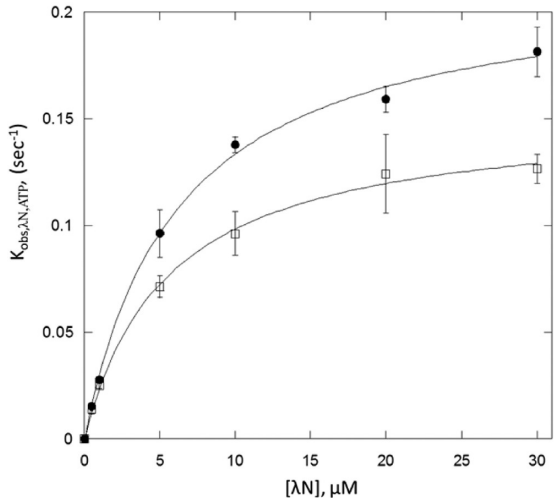

Figure 4. (A) Amino acid sequences of the λN protein used to monitor peptide bond cleavage by WT ELon. A FRET pair of abz/nitrotyrosine was used in both λN proteins. Both sequences contain the same internal fluorescence quenching pair: NO_2Tyr which quenches the fluorescence of Abz in the intact substrate, though the length between the two are different, with two cleavage sites between the fluorescent pair in FRλN001. ELon cleavage sites between the fluorescent pair are underlined. Upon peptide bond cleavage, separation of NO_2Tyr from Abz allows the detection of fluorescence emission generated by the latter at excitation 320 nm and emission 420 nm. (B) Steady-state kinetics of ATP-dependent hydrolysis of FRλN001 versus FRλN006 cleavage by WT ELon. The steady-state rate constants ($k_{obs\lambda N,ATP}$) of protein hydrolysis with varying concentrations of FRλN001 (●) and FRλN006 (□) were determined using the continuous fluorescence based proteinase assay as described in Materials and Methods. The $k_{obs\lambda N,ATP}$ values, determined by dividing reaction rates with enzyme monomer concentration, were plotted as a function of peptide concentration. The data were best fit with eq 3 to yield the kinetic parameters summarized in Table 1. The fit of the data is illustrated by the solid lines. Error bars show the experimental standard deviations of at least three independent trials from the averaged values.

products, the lack of product detected prior to the 1 s time point suggests the presence of lag kinetics in the reaction. However, the apparent lag phase in product detection could have also been attributed to the detection limit of the technique. Therefore, the stopped flow kinetic techniques described below were used to further characterize the first four seconds of the degradation reactions.

Fluorescently Labeled λN as a Substrate of ELon. To quantify the ATP-dependent peptidase activity of Lon, fluorogenic decapeptide substrates containing different regions of λN, each containing a Lon cleavage site, were previously generated.[40] Each intact peptide substrate contained a nitrotyrosine (NO_2Tyr) at the N-terminal and a lysine-conjugated anthranilamide (Abz) group at the epsilon amino side chain such that the fluorescence emission signal of Abz (λ_{ex} = 320 nm, λ_{em} = 420 nm) was internally quenched by nitrotyrosine due to proximity of the two moieties.[39] Upon cleavage by Lon, the two chromophores separate from one another, leading to an increase in the Abz fluorescence over time, thereby allowing for the determination the kinetic parameters of the peptidase reaction. In this study, we utilized the same strategy to monitor the cleavage of the N- versus the C-terminal cleavage of λN by ELon in the presence of ATP and independently AMPPNP. Two λN constructs were generated, one with two Lon cleavage sites flanked by NO_2Tyr and Abz at the amino end, and one with one Lon cleavage site flanked by the same set of chromophores at the carboxyl end (Figure 4A). These were generated by chemical synthesis without any his-tag. Since Trp also internally quenches the fluorescence of Abz, the intrinsic Trp residues in λN were replaced with Phe to ensure the observed changes in Abz signal were attributed to peptide bond cleavage. The resulting N- versus C- labeled λN substrates are referred to as FRλN001 and FRλN006, respectively. Due to the placement of the Abz-NO_2Tyr dye pair, the cleavage of A30-K31 or L40-N41 will be detected in FRλN001 and the cleavage of L93-S94 will be detected in FRλN006. In a previous study, the k_{cat} and K_m of each Lon cleavage site in λN were determined in fluorogenic decapeptides containing λN sequence flanking each site.[40] The cleavage sites at A30-K31, L40-N41, and L93-S94 have comparable k_{cat} values. Since A30-K31 and L40-N41 are closer to the N-terminal whereas L93-S94 is closer to the C-terminal of λN, we place the Abz-NO_2Tyr dye pair in FRλN001 to detect peptide bond cleavage at the N-terminal through monitoring the cleavage of either

dx.doi.org/10.1021/bi4008319 | Biochemistry 2013, 52, 5629−5644

Table 1. Kinetic Parameters for Protein Degradation of λN by WT ELon

	ATP steady-state		ATP pre-steady-state		AMPPNP pre-steady-state	
	$k_{cat\lambda N,ATP}$ (s^{-1})	K_m (μM)	$k_{obs\lambda N,\ ATP}$ (s^{-1})	$k_{lag\lambda N,\ ATP}$ (s^{-1})	$k_{obs\lambda N,AMPPNP}$ (s^{-1})	$k_{lag\lambda N,AMPPNP}$ (s^{-1})
FRλN001	0.22 ± 0.06	6.12 ± 0.53	0.11 ± 0.02	0.77 ± 0.08	0.0010 ± 0.0004	0.025 ± 0.004
FRλN006	0.15 ± 0.01	5.55 ± 0.50	0.08 ± 0.01	0.87 ± 0.12	0.0009 ± 0.0002	0.042 ± 0.008

A30-K31 or L40-N41. The cleavage of the C-terminal of λN will be detected by the separation of the dye pair flanking the L93-S94 in FRλN006.

When excited at 320 nm, both FRλN001 and FRλN006 emitted maximum fluorescence signal at ∼415 nm. Upon incubation with ELon and ATP, the signal intensity of FRλN001 and FRλN006 increased by 38 170 counts and 108 930 counts, respectively (see Supporting Information, S4). The difference in the signal intensity was attributed to the difference in the separation distance between NO_2Tyr and Abz in the two substrates. In FRλN001, NO_2Tyr was 16 residues from Lys(Abz), whereas in FRλN006, NO_2Tyr was 9 residues apart from Lys(Abz). Therefore the Abz moiety in FRλN006 had a lower intrinsic Abz fluorescence and was more effectively quenched. Using the fluorogenic assay described above, the $k_{cat\lambda N,ATP}$ and K_m values for the cleavage of the N-terminal in FRλN001 and C-terminal of FRλN006 at 1 mM [ATP] were determined by fitting the data that related the rate constant of peptide bond cleavage ($k_{obs\lambda N,ATP}$) with the indicated [substrate]. The plots shown in Figure 4B fit well with eq 3 to provide the values summarized in Table 1. Within experimental deviation, the $k_{cat\lambda N,ATP}$ and K_m values of both substrates are comparable. The detection of comparable $k_{cat\lambda N,ATP}$ and K_m values for the cleavage of both sites indicated the same rate-limiting step occurred in both degradation reactions.

One technical issue associated with the fluorogenic assay described here is the presence of an inner filter effect at high substrate concentrations.[45] To overcome this, a substrate cocktail containing 10% of the fluorescently labeled λN was mixed with 90% of unlabeled λN to make up the desirable substrate concentration for the assay. This approach was successfully used in the past to determine the kinetics of peptide bond cleavage in synthetic peptides.[40] In this study, controls were performed to ensure that the rate of peptide bond cleavage in the 10% labeled substrate was the same as the 100% labeled substrate using a substrate concentration that did not suffer from inner filter effect (see Supporting Information, S5). The substrate cocktail is referred to as λN001A and λN006A, respectively. They are used in the pre-steady-state stopped flow assays described below.

Pre-Steady-State Stopped Flow Time Courses of Peptide Bond Cleavage in λN under Pseudo First Order Conditions. To gain insights into the rate-limiting step in the ATP-dependent degradation of λN001A and λN006A, the cleavage of the NO_2Tyr/Abz-labeled site in λN001A and λN006A were monitored under excess [substrate] over [Lon] (∼2-fold $K_{m,\lambda N}$, λN; >10-fold $K_{d,\lambda N}$, λN) in the presence of 1 mM ATP (Figure 5A) or AMPPNP (Figure 5B) using a stopped-flow apparatus. Lag kinetics were detected in both reactions. Fitting the respective time courses with eq 4 yielded the kinetic parameters summarized in Table 1. The $k_{obs\lambda N,ATP}$ and $k_{obs\lambda N,AMPPNP}$ values correspond to the steady-state rate constant of the cleavage of the labeled site at 8 μM of λN001A or λN006A. The k_{lag} values reflect the rate constant for the transition of the slow to the fast phase of the time course. The $k_{lag\lambda N,ATP}$ values for the ATP-dependent cleavage reactions are between 20- and 35-fold higher than the $k_{lag\lambda N,AMPPNP}$ obtained for the AMPPNP-dependent reactions. A ∼10-fold lower ratio in the $k_{lag\lambda N,AMPPNP}$ of AMPPNP- versus the $k_{lag\lambda N,ATP}$ ATP-dependent cleavage of a decapeptide containing residues 89−98 of λN (the labeled site in FRλN006) was previously detected.[43] Taken together, a more pronounced dependency on the ATPase activity in k_{lag} for the same scissile site (flanking residues 89−98) in full-length λN versus the decapeptide was observed, suggesting that the length and/or presence of multiple Lon cleavage sites decreases the magnitude of k_{lag} in peptide bond cleavage. The detection of lag kinetics in both reactions could be attributed to the buildup of the same enzyme intermediate before peptide bond cleavage occurs, or that the separation of the fluorescent donor and acceptor in the hydrolyzed λN products awaits the complete degradation of the entire substrate, which constitutes the rate-limiting step. The latter possibility was deemed unlikely because no hydrolyzed peptide products or partially digested λN were detected within the same time frame when the degradation reactions were quenched with denaturants to release enzyme bound λN products (see Supporting Information S6). The lag kinetic profiles detected in the cleavage of λN001A and λN006A are consistent with the rate-limiting substrate delivery step previously detected in the ATP- and AMPPNP-dependent cleavage of a fluorogenic peptide constituting residues 89−98 of λN.[43] The reciprocal of k_{lag} provides an estimate for the duration of the lag phase (τ)[46] which is 1.3 s for λN001A and 1.15 s for λN006A in the presence of ATP. In the presence of AMPPNP, the τ values are 40 and 24 s for λN001A and λN006A, respectively. As further discerned in Table 1, the k_{lag} and k_{obs} of the ATP- and, independently, AMPPNP-dependent cleavage of λN001A are comparable to the values obtained for λN006A, indicating that the same rate-limiting step dictates the cleavage of both sites.

Dansylated λN as Reporters to Monitor Translocation of N- versus C-Terminal of λN and the Utilization of S679W ELon. In a previous study, the delivery of the synthetic peptide substrate constituting residues 89−98 of λN to the proteolytic site of ELon was detected by FRET, where the Trp in S679W ELon served as the donor and the dansylated peptide substrate acted as the acceptor.[47] In S679W ELon, the proteolytic site Ser was mutated to Trp such that the mutant possessed WT-like ATPase activity but was proteolytically inactive. It was discovered that the FRET signal generated from S679W interacting with the dansylated peptide substrate occurred prior to peptide bond cleavage. As such, the timing of their delivery to the protoelytic site could be monitored by the FRET signal generated from exciting the Trps in S679W ELon and detecting dansyl emission. Capitalizing on this technology, we generated the three dansylated λN constructs shown in Figure 6A. The three constructs differ by the location of a dansylated Cys inserted upstream and downstream of the Lon cleavage sites at residues A30-K31, L40-N41, and L93-S94 The location of the dansylated sites are illustrated in Figure 6A. DansylλN001 contains a dansyl label at position 26, 4 residues

dx.doi.org/10.1021/bi4008319 | Biochemistry 2013, 52, 5629−5644

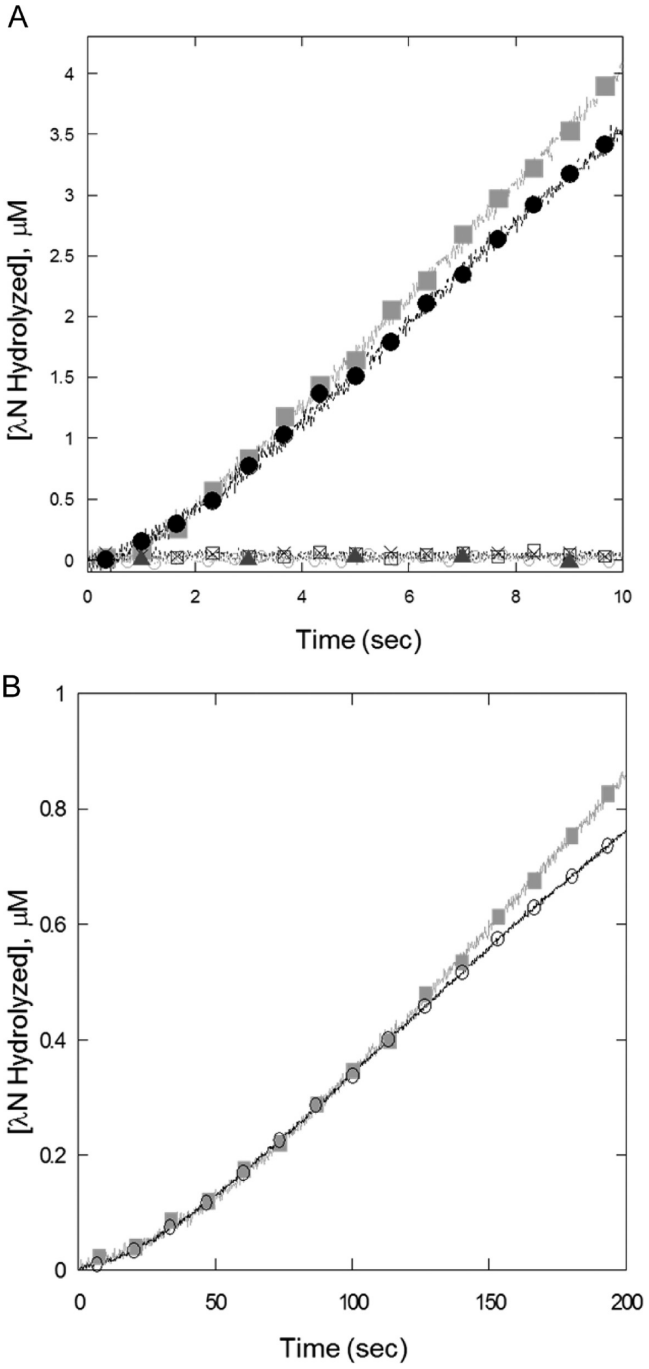

Figure 5. Stopped-flow analysis of ATP-dependent FRλN cleavage by WT ELon under excess FRλN conditions. (A) 5 μM WT ELon was incubated with 8 μM λN001A with no nucleotide (○), 1 mM ADP (□), or 1 mM ATP (■), or 8 μM λN006A with no nucleotide (×), 1 mM ADP (▲), or 1 mM ATP (●). (B) 5 μM WT ELon was incubated with 10 μM λN001A (■) or 10 μM λN006A (○) with 1 mM AMPPNP. The fluorescent changes associated with peptide cleavage were converted to product concentrations as described in Materials and Methods. Each time course shown is an average of 4 traces. The traces with ATP and AMPPNP were set to eq 4 to determine the kinetic parameters listed in Table 1. No change in fluorescence was observed without nucleotide or with ADP.

downstream from the Lon cleavage site at A30-K31, and is the furthest away from the C-terminal. DansylλN002 contains a dansyl label at position 42, 1 residue upstream from the Lon cleavage site L40-N41, and is 14 residues closer than dansylλN001 to the C-terminal. The fluorescent label of dansylλN006 is located at position 99, 5 residues from the Lon cleavage site at L93-S94, and is the closest to the C-terminal. Each dansylated site was located at the vicinity of a different Lon cleavage site, which differs by their respective locations from the C-terminal containing residues 99−107. As such, the timing of their delivery to the protoelytic site could be monitored by the FRET signal generated from exciting the Trps in S679W Lon and detecting dansyl emission.

The Trp fluorescence of S679W ELon was nonspecifically quenched by dansyl glutamic acid, but greater decrease in Trp fluorescence was detected in reactions containing any one of the dansylated λN proteins (see Supporting Information S7). No change in Trp fluorescence was detected when Lon was incubated with unlabeled λN001, λN002, or λN006 (data not shown). A decrease in Trp fluorescence was accompanied by an increase in dansyl fluorescence in a reaction containing S679W ELon, dansylλN, and ATP, indicating the presence of FRET. Since Trps are only present in Lon, the decrease in Trp fluorescence accompanied by the increase in dansyl fluorescence upon excitation of Trp at 295 nm demonstrates the existence of FRET signal between S679W ELon and dansylated λN. Furthermore, both the decrease in Trp and increase in dansyl fluorescence exhibit dependency on the concentration of dansylλN incubated with S679W ELon. These results indicate that the binding interaction between S679W ELon and the respective dansylated λN at the specific site can be monitored by FRET.

The S679W ELon mutant contains 4 Trp residues, with the 679W located at the protoelytic site.[47] To determine the extent to which 679W contributed to the FRET signal, the stopped flow fluorescence time courses of dansylλN001, dansylλN002, and dansylλN006 interacting with S679W versus S679A ELon in the presence of 0.5 mM ATP were monitored. For comparison, the time courses of dansylλN001, dansylλ002, and dansylλN006 mixed with S679W ELon in the absence of any nucleotide and in the presence of 0.5 mM ADP were also obtained. The time courses for the increases in dansyl fluorescence are shown in Figure 6B and the concomitant decreases in Trp fluorescence are shown in Figures 6C, D, and E. According to the data, the Trp fluorescence in S679A was affected by the presence of the dansylated λN constructs, but these changes did not significantly affect the dansyl signal. Although a small amount of change in dansyl fluorescence was detected in the S679A reaction, the most noticeable changes in dansyl as well as Trp fluorescence were detected in the S679W time courses. Taken together, these results showed that the FRET signal was generated primarily by 679W interacting with the dansyl label in λN in an ATP-dependent manner.

Pre-Steady-State FRET Time Course for the Delivery of a Specific Dansylated Site in λN under Pseudo First Order Conditions. A unidirectional substrate translocation process has been found to exist in ATP-dependent protease complexes ClpXP and ClpAP, but has yet to be shown to exist in Lon.[18,24,30,48,49] To evaluate the existence of directionality in the delivery of substrate to the proteolytic site of ELon, we determined the order by which dansylλN001, dansylλN002, and dansylλN006 interacted with S679W ELon through monitoring the duration needed for each construct to obtain maximum FRET signal between the dansyl label and 679W Trp. The time courses for S679W ELon interacting with dansylλN001, dansylλN002 and dansylλN006 in the presence of ATP or AMPPNP were obtained by exciting the reactions at

dx.doi.org/10.1021/bi4008319 | Biochemistry 2013, 52, 5629−5644

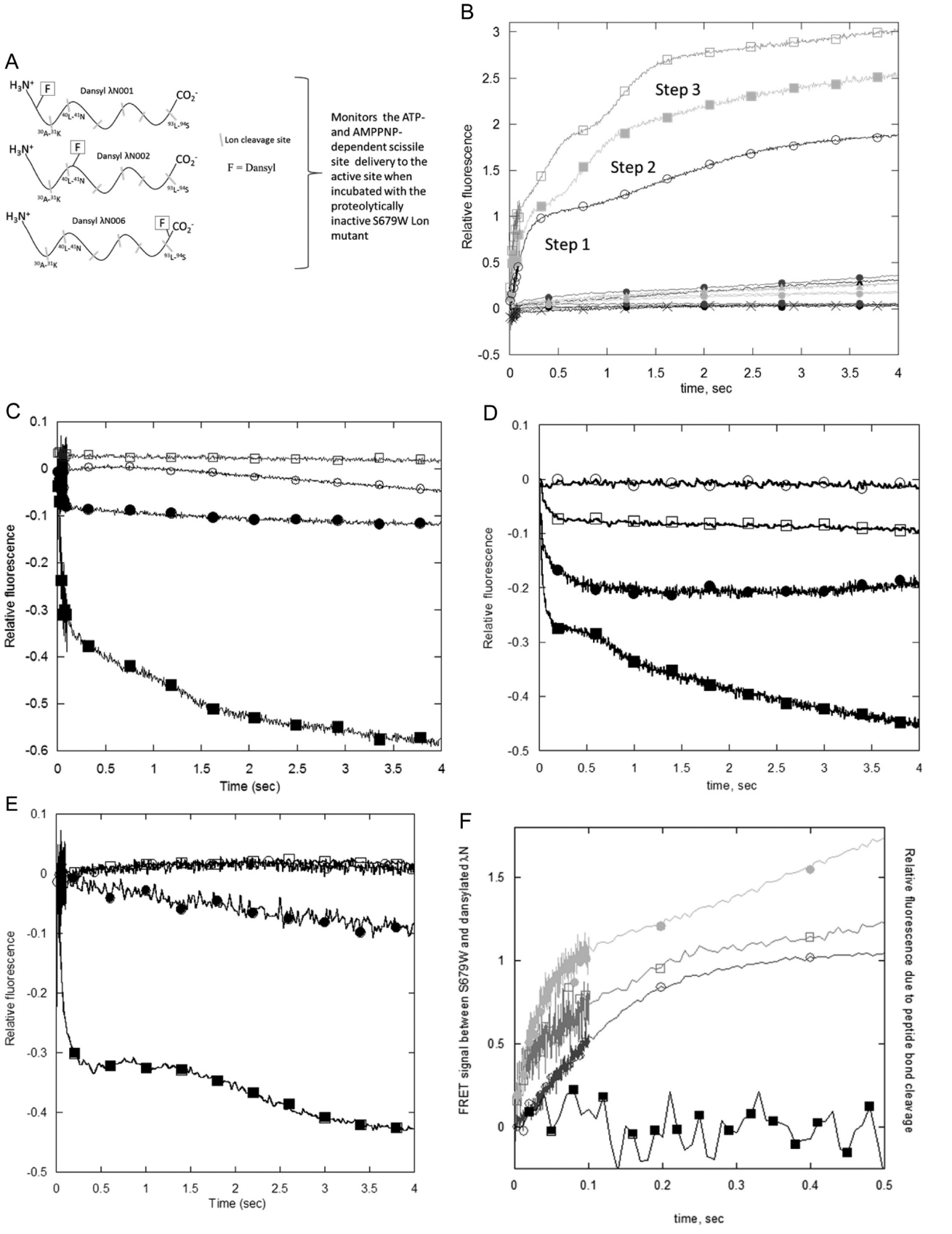

Figure 6. (A) Design of fluorescent λN protein used to monitor degradation and translocation by ELon. (B) Stopped-flow analysis of ATP-dependent dansylλN delivery by S679W and S679A ELon under excess dansylλN conditions. 5 μM S679W ELon was incubated with 0.5 mM ATP and 10 μM dansylλN001 (○), dansylλN002 (□), or dansylλN006 (●). 5 μM S679W ELon was incubated with 1 mM ADP and dansyl λN001 (■, dark gray), no nucleotide and dansylλN001 (●, dark gray), 0.5 mM ADP and dansylλN002 (■, light gray), no nucleotide and dansylλN002 (●, light gray), 0.5 mM ADP and dansylλN006 (■, black) or no nucleotide (■, black). 5 μM S679A ELon was incubated with 10 μM dansylλN001 (▲, dark

dx.doi.org/10.1021/bi4008319 | *Biochemistry* 2013, 52, 5629−5644

Figure 6. continued

gray), dansylλN002 (▲, light gray), or dansylλN006 (▲, black) and 0.5 mM ATP. The reaction was excited at 295 nm and dansyl fluorescence was monitored using a 450 nm long-pass filter. (C, D, E) The reactions described in part B were also monitored for changes in tryptophan fluorescence by excitation at 295 nm and detecting emission with a 340 nm bandpass filter. 5 μM S679W ELon was incubated with 10 μM dansylλN001 (C), dansylλN002 (D), or dansylλN (E) with no nucleotide (□), 0.5 mM ADP (○), or 0.5 mM ATP (■). 5 μM S679A ELon was incubated with 10 μM dansylλN001 with 0.5 mM ATP (●). (F) Pre-steady-state time course of dansylλN delivery. The first 0.5 s of the ATP-dependent reactions seen in part A were fit with eq 5 to yield $k_{1,FRET,ATP}$ values for dansylλN001 (●), dansylλN002 (□), and dansylλN006 (○) as summarized in Table 2. For comparison, cleavage of λN006A (■) by WT ELon with ATP is also shown. The right y-axis shows relative fluorescence due to peptide bond cleavage.

295 nm and detecting fluorescence intensity at >450 nm using a cutoff filter. The Förster distance for the Trp donor and dansyl acceptor is between 21 and 24 Å.[50] According to the crystal structure of *Thermococcus onnurineus* Lon, which shows sequence homology with the protease domain of *E. coli* Lon, the active sites in each subunit are 32 Å apart from each other, and 28 Å from the center of the translocation channel.[51] Therefore, the FRET approach employed in this study detected the kinetic events occurring within the Förster distance set by the donor−acceptor pair, which was from the end of the translocation channel to the proteolytic site of ELon. Kinetic information concerning the initiation of substrate delivery to the active site that occurred beyond the specified Förster distance would not have been recorded. Given this constraint, the conclusion drawn from this study reveals the timing and kinetic coordination between the final stage of substrate delivery to the protoelytic site and peptide bond cleavage. Since a scissile site has to reach the protoelytic site and bind productively for peptide bond cleavage to occur, the lag rate constants and the corresponding τ values $(1/k_{lag})$, which defined the duration of the lag phase, were used as the end point of substrate delivery.

In theory, the amplitude of the changes in FRET signal could be used to calculate the Förster distance between a donor and an acceptor. However, both trp and dansyl are environmentally sensitive dyes. The FRET efficiency between the dansyl group and Trp will vary due to different peptide sequences surrounding each dansyl probe in the three dansyl λN constructs, thereby obscuring the utilization of the FRET amplitude to obtain distance information. Moreover, once bound to the active site of Lon, conformational changes in enzyme may occur to cause additional changes in the orientation of dansyl and Trp, thereby producing further changes in FRET kinetics. Each kinetic step could be attributed to the translational movement or spatial orientation of the fluorescent probes due to enzyme conformational changes. As pointed out in Methods and Materials, in the acquisition of the FRET time courses, different detector sensitivity settings were used to optimize signal detection. Given these considerations, the amplitudes of the FRET time courses could not be directly compared to obtain information on distances. Only kinetic parameters were extracted from the FRET time courses to deduce the order of scissile site delivery in λN to 679W of the ELon mutant.

Figure 6B presents the standardized stopped flow time courses (representative of at least three independent experiments) of S679W ELon mixed with near-saturating concentration (~2-fold K_m, and >10-fold K_d) of dansylated λN001, λN002, and λN006, at saturating [ATP] (10-fold K_m). The y-axis reports the FRET signal intensity generated from each reaction. As the reactions were excited at the Trp wavelength (295 nm) and changes in fluorescence intensity were recorded at the dansyl excitation wavelength, the stepwise increases in the dansyl fluorescence are assigned to the FRET signal generated from the delivery of the respective dansylated site to 679W via translational movement and/or spatial orientation of the two groups due to conformational changes at the enzyme active site. It is discerned from the FRET time courses that the fluorescence probe located at residue 99 attains steady-state signal before the probe at residue 42 and then the probe at residue 26. The subsequent slow changes in FRET signal are assigned to the steady-state ATPase-mediated conformational changes in the enzyme's proteolytic site that affect the local environment of dansyl and 679W FRET interaction. This speculation is supported by a previous study showing that the proteolytic site of ELon interacted with a synthetic peptide containing residues 89−98 of λN differently in the presence of ATP versus ADP.[40] During the steady-state ATPase cycle, S679W is anticipated to undergo repeated cycles of conformational changes.

A comparison of the first 0.4 s of the ATP-dependent FRET time courses for the three dansylated λN constructs is shown in Figure 6F. The FRET signal originating from dansyl approaching 679W seems to initiate at dansylλN001, followed by dansylλN002 and then dansylλN006. Fitting the data spanning the first 0.4 s with eq 5 yields a rate constants, as seen in Table 2, $k_{1,FRET,ATP}$ of 16.63 ± 0.46 s^{-1} for dansylλN001, 8.91 ± 0.47 s^{-1} for dansylλN002, and 5.82 ± 0.13 s^{-1} for dansylλN006, respectively. This data suggests that within the detection limit of the Förster distance of the dansyl/Trp FRET dye pair, the N-terminal (represented by dansylλN001) begins to approach 679W before the other two sites, but it takes three steps spanning ~1.5 s to obtain steady-state FRET, implying that this is the last site to reach 679W. By contrast, attainment of FRET steady-state is completed in dansylλN002 in two steps within 1 s and in dansylλN006 in one step within 0.5 s. As extrapolated from the $k_{lag\lambda N,ATP}$ of λN006A and λN001A found in Table 1 and discussed earlier, the duration of the lag phase (τ[46]) in peptide bond cleavage amounts to 1.15 to 1.3 s. This lag phase is attributed to the buildup of an enzyme intermediate needed to initiate peptide bond cleavage. The termination of the lag phase therefore sets the end point for considering the FRET signals associated with substrate delivery prior to peptide bond cleavage. Comparing the FRET signals associated with S679W interacting with any of the dansylated Cys in

Table 2. Kinetic Constants for DansylλN Interacting with S679W

	$k_{1,FRET,AMPPNP}$ (s^{-1})	$k_{2,FRET,AMPPNP}$ (s^{-1})	$k_{1,FRET,ATP}$ (s^{-1})
DansylλN001	0.337 ± 0.029	0.028 ± 0.003	16.63 ± 0.46
DansylλN002	0.404 ± 0.059	0.038 ± 0.006	8.91 ± 0.47
DansylλN006	0.633 ± 0.035	0.083 ± 0.009	5.82 ± 0.13

dx.doi.org/10.1021/bi4008319 | *Biochemistry* 2013, 52, 5629−5644

dansylλN001, dansylλN002, and dansylλN006 within the first 1.15−1.3 s (τ) of the time courses shown in Figure 6B reveals a maximum increase in signal observed in the reactions containing dansylλN002 or dansylλN006. An "almost completed" increase in FRET signal was detected in the time course containing dansylλN001, whose dansyl label was the furthest away from the C-terminal of the substrate. As the lag phase of the cleavage of peptide bond in λN006A or λN001A spans approximately the duration needed to complete the delivery of dansylλN001, we propose that the kinetic data supports a mechanism in which the initiation of peptide bond cleavage occurs after almost complete delivery of the scissile sites in λN substrate to the active site in ELon. It is possible that the observed FRET signal could also be partially attributed to changes in the orientation of the dansyl label with respect to 679W once it is delivered into the proteolytic chamber. As such, one or more of the "steps" detected in the reactions with dansylλN001 and dansylλN002 could be caused by conformational changes in the proteolytic site that lead to changes in the time courses. As ELon is a homohexamer, it is possible that once the dansylated substrate is delivered into the proteolytic chamber, the fluorescent label is close enough to two 679W active sites (one on each enzyme subunit) to allow significant FRET to occur. The kinetic experiments described in this study could not eliminate such a possibility. Nevertheless, the FRET time courses recorded in this study still allow for the comparison of the kinetics by which different regions of λN (labeled with dansyl) approach the proteolytic site prior to their cleavage. Additional experimentation will be required to further characterize the mechanistic basis for the stepwise changes in FRET signals.

Pre-Steady-State Kinetic of the λN Stimulated ATPase Activity of ELon. Attempts to fit the ATP-dependent delivery time courses shown in Figure 6B with traditional one to three exponential functions were unsuccessful. Graphically, the time course of each reaction bears a resemblance to the pre-steady-state time course of the ATPase activity of ELon obtained in the presence of a synthetic peptide containing residues 89−98 of λN.[52] Therefore, it is plausible that each "step-like" phase of the time course is coordinated with an ATPase cycle. To evaluate such a possibility, the time courses of ATP hydrolysis catalyzed by WT ELon stimulated by 8 μM of unlabeled λN001, which contains a Cys insertion at position 26, and λN006, which contains a Cys insertion at position 99, were determined. Figure 7A shows the time courses of the ATPase reactions obtained up to 2 s. Both time courses show a rapid burst followed by a transient plateau and then a steady-state increase in ATP hydrolysis. This observation matches with the previously published results obtained using a decapeptide containing residues 89−98 of λN.[52] Therefore, the substrate-stimulated ATPase activity of ELon appears insensitive to the size or number of Lon cleavage sites present in a substrate. Figure 7B compares the time course of ATP hydrolysis obtained up to 0.4 s. Fitting the data to the single exponential function yields the kinetic parameters found in Table 3. The burst rate constant, k_{burst}, for ATP hydrolysis is 11.54 ± 1.79 s^{-1} in the presence of λN001, and 6.49 ± 1.08 s^{-1} in the presence of λN006. The burst amplitude, which reflects the stoichiometry of ADP generated per enzyme monomer during the first enzyme turnover, is 2.61 ± 0.16 and 2.81 ± 0.18 for λN001 and λN006, respectively. Since 5 μM of ELon monomer was used in the ATPase reactions, the observed ~50% pre-steady-state burst in ATP hydrolysis suggests half-site reactivity, which agrees with our previous finding when a peptide rather than λN was used as substrate.[52] Despite an apparent 2-fold difference in the two k_{burst} values, the error bars shown in Figure 7B reveal

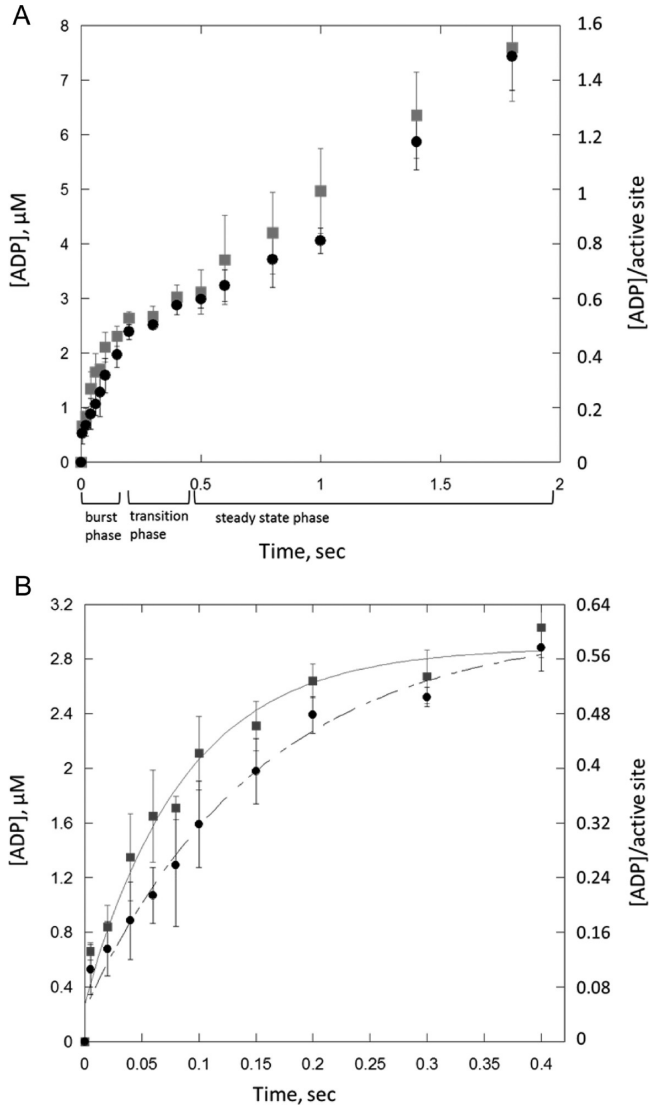

Figure 7. Pre-steady time courses of ATP hydrolysis by ELon. (A) [α-^{32}P] ATP (200 μM) was incubated with 5 μM monomeric ELon in the present of 8 μM λN001 (■) or λN006 (●), and reactions were quenched with acid at the indicated times. The concentrations of [α-^{32}P] ADP generated in the reactions were determined by TLC followed by PhosphorImaging as described in the Material and Methods. The values on the y axis were obtained by dividing the [ADP] produced by 5 μM monomeric ELon, which reflects the mole equivalent of ADP produced per Lon monomer. (B) Time points from 0 to 400 ms of λN001 (■) or λN006 (●) were fit with eq 7 to yield the kinetic parameters summarized in Table 3.

Table 3. ATPase Activity of WT ELon Stimulated by λN001 and λN006

	$k_{obs,ATPase}$ (s^{-1})[a]	k_{burst} (s^{-1})[b]	burst amplitude, (μM)[b]
λN001	0.67 ± 0.045	11.54 ± 1.79	2.61 ± 0.16
λN006	0.72 ± 0.085	6.49 ± 1.08	2.81 ± 0.18

[a]These values were obtained by fitting the data in Figure 8A from 600 ms to 1.8 s with eq 8. [b]These values were obtained by fitting the acid-quenched time courses (0−400 ms) of ATP hydrolysis that are shown in Figure 8B with eq 7.

dx.doi.org/10.1021/bi4008319 | Biochemistry 2013, 52, 5629−5644

that the burst kinetics displayed by the two reactions are comparable. Therefore the k_{burst} of λN-stimulated ATPase is between 6.49 and 11.54 s^{-1}, which is similar to the $k_{1,FRET,ATP}$ values obtained in the fitting of the first 0.4 s of the ATP-dependent FRET time courses shown in Figure 6F. This result suggests that the initial burst of ATPase of ELon is coordinated with the first phase of substrate delivery.

AMPPNP-Dependent Delivery of λN to 679W. As ELon catalyzed the delivery of the synthetic decapeptide containing residues 89−98 of λN to the active site of ELon in the presence of AMPPNP,[47] the kinetics of ELon delivering dansylλN001, dansylλN002, and dansylλN006 in the presence of this nonhydrolyzable ATP analog were also examined by the FRET technique. Figure 8 shows the time courses of the

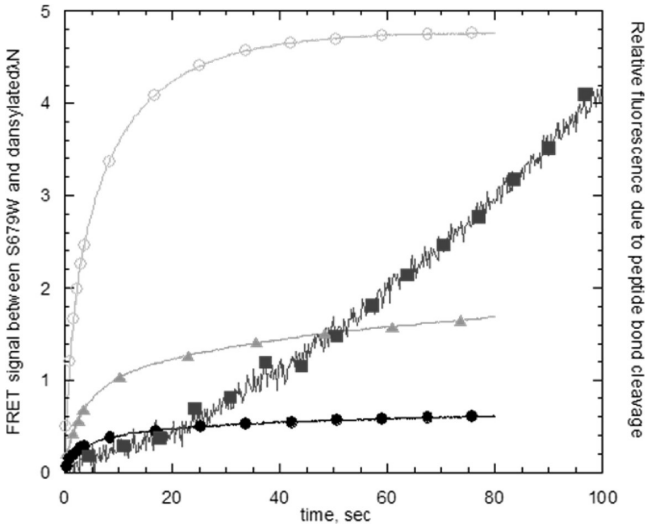

Figure 8. Substrate delivery to S679W ELon active site can be monitored using the dansylλN protein and AMPPNP. (A) 5 μM S679W ELon was incubated with 10 μM dansylλN001 (▲), dansylλN002 (●), or dansylλN006 (○) and 1 mM AMPPNP. The left *y*-axis shows relative FRET signal between the S679W ELon and dansylated λN. Time courses were fit with eq 6 to yield the kinetic parameters summarized in Table 2. Cleavage of λN001A (■) by WT ELon with AMPPNP is also shown for comparison. The right *y*-axis shows relative fluorescence due to peptide bond cleavage.

respective dansylated λN approaching 679W (representatives of at least three independent experiments). For comparison, the time course of the AMPPMP-dependent degradation of λN001A was also included. The *y*-axis reports the FRET signal intensity generated from each reaction. Unlike the ATP-dependent time courses shown in Figure 6B, the AMPPNP-dependent time courses are best fit with the double exponential function (eq 6) to yield the rate constants shown in Table 2. Both the $k_{1,FRET,AMPPNP}$ and $k_{2,FRET,AMPPNP}$ values follow the same descending order in which dansylλN006 > dansylλN002 > dansylλN001, suggesting that C-terminal end of λN approaches and reaches 679W first. This result differs from the ATP-dependent reactions (Figure 6B) by the terminal of λN that initiates movement toward 679W. In both cases, however, the C-terminal of λN is the first to reach 679W.

The detection of two observed rate constants for each AMPPNP-dependent time course indicates the presence of at least two steps in the delivery event. The observation of a two-step substrate delivery step is reminiscent of our earlier discovery that the ATP- or AMPPNP-dependent delivery of the dansylated peptide containing residues 89−98 of λN to S679W ELon involved the formation of a S679W:nucleotide:dansylated substrate complex followed by a second conformational change in the complex attributed to the delivery of the dansylated substrate to the proteolytic site at 679W.[47] As revealed by the standard errors of the fits, the $k_{2,FRET,AMPPNP}$ values of dansylλN001 and dansylλN002 are comparable to the $k_{lagλN,AMPPNP}$ of peptide bond cleavage in FRλN001 and FRλN002 (see Table 1), suggesting $k_{2,FRET,AMPPNP}$ of dansylλN001 or 002 constitutes the lag of peptide bond cleavage in the FRλN constructs. By contrast, the $k_{2,FRET,AMPPNP}$ of dansylλN006 is approximately 2- to 3-fold higher that the $k_{lagλN,AMPPNP}$ of the FRλN constructs and the $k_{2,FRET,AMPPNP}$ of dansylλN001 or dansylλN002, indicating that the step corresponding to $k_{2,FRET,AMPPNP}$ in dansylλN006 occurs faster. As FRET signal is generated from the dansyl label in λN approaching 679W in Lon mutant, we conclude that, in the presence of AMPPNP, the C-terminal of λN, which is represented by dansylλN006, approaches the proteolytic site of ELon before the N-terminal, which is represented by dansylλN001 and dansylλN002. The similarity in the $k_{2,FRET,AMPPNP}$ of dansylλN001 and dansylλN002 could be attributed to the location of these two probes being not far apart enough to detect noticeable difference in the kinetic experiment. Additional kinetic studies which involve determining the entire kinetic mechanism of λN translocation will be required to further define the molecular natures of the two kinetic steps detected in the AMPPNP-dependent reactions.

■ DISCUSSION

Processive protein degradation is a common feature found in ATP-dependent proteases. Protein substrates are degraded into peptides ranging from 5 to 20 amino acids long without the generation of partially digested substrates. The study of processivity has been primarily conducted in the hererosubunit ATP-dependent proteases using FRET techniques.[24,30] In these studies, Cys mutations were introduced into model substrate and enzyme subunits for chemical attachment of fluorescence donor and acceptor dyes containing overlapping spectral properties. The model substrates typically contain an enzyme recognition tag such as an ssrA tag to direct initiation of substrate binding to the ATPase subunit of the protease complex. Using this approach, the kinetics of substrate unfolding, translocation, and peptide bond cleavage have been obtained.[30,31] In Lon protease, alkylation of Cys residues leads to enzyme inactivation.[23] Therefore, the FRET approach used for studying the processive mechanism of the Clp complexes cannot be used on Lon. As an alternative, the methodologies previously used to study the kinetic mechanism of ATP-dependent delivery to the active site and cleavage of the decapeptide containing residues 89−98 of λN were adapted.[47] In this study, two synthetic λN variants, each lacking intrinsic Trp residues, were labeled with the internally fluorescent quenching group, NO_2Tyr and Lys(Abz), such that the kinetics of peptide bond cleavage occurring at each end of λN could be quantified. These two sites were separated by at least 50 residues. Independently, "*trp*less" λN variants containing a unique Cys at sites proximal to the target scissile sites were labeled with dansyl to generate a site-specific labeled substrate that allowed for the detection of substrate delivery with the proteolytically inactive ELon mutant S679W, which possessed WT-like ATPase activity. Comparing the time courses of specific site cleavage versus delivery revealed that the three

dx.doi.org/10.1021/bi4008319 | *Biochemistry* 2013, 52, 5629−5644

dansylated sites were delivered to the 679W site in ELon before any peptide bond cleavage occurs.

In Lon, a naturally occurring substrate recognition tag has not been identified in physiological substrates. Gur and Sauer have identified hydrophobic peptide sequences that directed the degradation of non-natural substrates by Lon, but the physiological relevance of these peptide recognition tags was not clear.[53] A review on the degradation profiles of physiological substrates of bacterial Lon reveals that recognition elements other than hydrophobic patches in these substrates can target proteins for degradation, and thus far, no consensus recognition tag has been identified for the recognition and degradation of physiological substrates of Lon.[54] Given these considerations, we chose the λN protein, which is the endogenous protein substrate of ELon,[25] to study the processive protein degradation mechanism of Lon. Structural studies have shown that full length and truncated λN variants do not contain defined secondary structures.[35,36] The kinetic coordination between the delivery to the active site and cleavage of different regions of λN can thus be directly monitored without interferences from substrate unfolding. Based on the rate constants summarized in Tables 1 and 2 and the results shown in Figures 6B and 8, the order of scissile site delivery occurs from the C- to N-terminal. Although residues 99−107 contribute to the binding affinity of λN by ELon, it is currently not clear the extent to which the directionality of substrate delivery is affected by these residues, as λN lacking these residues was still degraded by ELon, albeit with lower efficiency than WT λN.

To evaluate the timing of peptide bond cleavage at different scissile sites in λN, an iTRAQ mass spectrometry experiment that allowed for the quantification of the degradation of different regions of λN was performed. The detection of comparable time courses in the generation of different hydrolyzed peptide products suggests that the different scissile sites in λN were cleaved with comparable timing during the reaction. This implication was corroborated by the kinetic results obtained for the cleavage of the two scissile sites at the N-terminal in FRλN001 and one scissile site at the C-terminal in FRλN006, which exhibited comparable kinetic parameters in their respective cleavages (Table 1). In an earlier study, the k_{cat} and K_m values for the ATP-dependent cleavage of the individual fluorescently labeled scissile sites of λN have been determined in decapeptides. Overall, the K_m as well as the k_{cat} values of the peptide analog of the same scissile site are larger than in full-length λN. The difference in K_m could be attributed to the ability of ELon to interact with multiple regions of λN, which results in an apparently >100-fold lower K_m of the substrate. As for the difference in the k_{cat} value, the synthetic peptide substrates are ∼10-fold shorter in length than λN. The observed reduction in the k_{cat} of λN cleavage obtained in this study could be attributed to the extra time needed to translocate the entire protein before initiation of peptide bond cleavage compared to the small peptides. In congruence with this finding was the detection of an "almost complete" delivery of the three dansylated sites in λN to the active site coinciding with the lag phase of the cleavage of the cognate sites in λN in the ATP- as well as AMPPNP-dependent reactions. Collectively these results also account for the observation that only completely digested peptide products are detected in a typical ATP-dependent λN degradation time course quenched with denaturant. As peptide cleavage only occurs after complete delivery of λN, any partially translocated λN would have been detected as undigested λN in SDS-PAGE. The observed concerted peptide bond cleavage occurring after almost complete translocation of the entire substrate has also been detected in other heterosubunit ATP-dependent proteases.[30] This result, however, contradicts the mechanism proposed by Choi and Licht, who observed that the extrusion of polypeptide substrate into the heterosubunit ATP-dependent protease ClpAP alternated with peptide bond cleavage events[55] and will require further investigation to reconcile the differences observed in these studies.

A unidirectional substrate translocation process has been found to exist in the Clp complexes, but has yet to be shown to exist in Lon.[18,24,48,49] Through comparing the kinetic time courses of the delivery of different regions of λN, represented by dansylλN001, dansylλN002, and dansylλN006, to the active site S679W in the presence of ATP and independently AMPPNP, the delivery of the scissile site beginning at the C-terminal was implicated. As no putative recognition peptide tag for Lon has been identified in λN, it is currently not clear if the region constituting residues 99−107, which affects substrate binding affinity, contributes to the directionality of substrate translocation. Since λN lacking residues 99−107 was also degraded processively by ELon, it is likely that internal region(s) within λN also participate in directing substrate translocation. As such, a more in-depth structure−function study on the translocation profile of λN by ELon will be needed. The kinetic approach described in this study will provide the conceptual and technological framework for completing such analysis.

In summary, we utilized a kinetic approach to demonstrate that the processive degradation of λN by ELon occurs via model 1 shown in Scheme 1. The transient kinetic data generated in this study reveals that the cleavage of the different scissile sites in λN occurs after the delivery of the protein substrate to the enzyme active site. The different scissile sites in λN are delivered at different times, but their subsequent cleavage encounter the same rate-limiting step. Despite the lack of a defined recognition peptide tag, the C-terminal of λN is delivered to the protoelytic site before the N-terminal. The residues located within positions 99−107 of λN contribute to the binding affinity of λN by ELon, but other residues beyond this region are also needed for substrate binding and translocation. Comparing the kinetic time courses of ATP- versus AMPPNP-dependent degradation and delivery of λN reveals that processive protein degradation requires ATP binding but not hydrolysis. However, ATP hydrolysis facilitates the efficiency of both events.

■ ASSOCIATED CONTENT

Supporting Information

Details of the λN degradations, iTRAQ, changes in fluorescence of FRλN, degradation of 100% FRλN versus 10% FRλN, detection of lag kinetics in a discontinuous assay, and emission scans of Trp/dansyl FRET. This material is available free of charge via the Internet at http://pubs.acs.org.

■ AUTHOR INFORMATION

Corresponding Author

*E-mail address: IXL13@CASE.EDU; phone: (216)368-6001; fax: (216)368-3006.

Present Address

Jennifer Fishovitz, Department of Chemistry and Biochemistry, University of Notre Dame, IN 46556−5670

Author Contributions

This work was completed in fulfillment of a summer undergraduate research project (Jonathan Huang).

Funding

This work was supported by a grant from NSF MCB-0919631 and a grant from NSF CHE-1213175.

Notes

The authors declare no competing financial interest.

■ ABBREVIATIONS:

Abz, anthranilamide; ADP, adenosine diphosphate; AMPPNP, adenylyl 5-imidodiphosphate; ATP, adenosine triphosphate; BCIP, 5-bromo-4-chloro-3′-indolyl phosphate *p*-toluidine salt; C-his-λN, 6x his tag at the carboxyl end of wild type λN sequence; Clp, caseinolytic protease complex; C-terminal, carboxyl terminal; DTT, dithiothreitol; FRET, fluorescence resonance energy transfer; FRλ001, a fluorescent protein substrate of Lon with a nitrotyrosine and anthranilamide at the amino end of λN; FRλN002, a fluorescent protein substrate of Lon with a nitrotyrosine and anthranilamide at the carboxyl end of λN; HEPES, N-2-hydroxyethylpiperazine-N′-ethanesulphonic acid; iTRAQ, isobaric tag for relative and absolute quantitation; KOAc, potassium acetate; KPi, potassium phosphate; λN, also known as λN protein, a λ phage protein; λN001A, a fluorescent protein substrate of Lon containing 10% FRλN001 and 90% λN001; λN001, cysteine at the 26th position of wild type λN; λN002, cysteine at the 42nd position of wild type λN; λN006A, a fluorescent protein substrate of Lon containing 10% FRλN006 and 90% λN006; λN006, cysteine at the 99th position of wild type λN; λNΔ1−34, truncated λN lacking the N-terminal; N-his-λNΔ99−107, truncated λN lacking the C-terminal; LC/MS/MS, liquid chromatography/mass spectrometry/mass spectrometry; $Mg(OAc)_2$, magnesium acetate; MW, molecular weight; NBT, nitro-blue tetrazolium chloride; NO_2Tyr, nitrotyrosine; N-terminal, amino terminal; PAGE, polyacrylamide gel electrophoresis; PEI-cellulose, polyethyleneimine-cellulose; PMT, photomultiplier tube; RQ/MS, chemical quench-flow mass spectrometry assay; SDS, sodium dodecyl sulfate; TBST, Tris-Buffered Saline with Tween 20; TCEP, tris(2-carboxyethyl)-phosphine; TLC, thin layer chromatography; Tris, 2-amino-2-(hydroxymethyl)-1,3-proanediol; WT, wild type; N-his-λN, 6x his tag at the amino end of wild type λN sequence

■ REFERENCES

(1) Rep, M., and Grivell, L. A. (1996) The role of protein degradation in mitochondrial function and biogenesis. *Curr. Genet. 30*, 367−380.

(2) Maurizi, M. R. (1992) Proteases and protein degradation in Escherichia coli. *Experientia 48*, 178−201.

(3) Suzuki, C. K., Rep, M., van Dijl, J. M., Suda, K., Grivell, L. A., and Schatz, G. (1997) ATP-dependent proteases that also chaperone protein biogenesis. *Trends Biochem. Sci. 22*, 118−123.

(4) Goldberg, A. L. (1992) The mechanism and functions of ATP-dependent proteases in bacterial and animal cells. *Eur. J. Biochem. 203*, 9−23.

(5) Gottesman, S., and Maurizi, M. R. (1992) Regulation by proteolysis: energy-dependent proteases and their targets. *Microbiol. Rev. 56*, 592−621.

(6) Kaser, M., and Langer, T. (2000) Protein degradation in mitochondria. *Semin. Cell Dev. Biol. 11*, 181−190.

(7) van Dyck, L., and Langer, T. (1999) ATP-dependent proteases controlling mitochondrial function in the yeast *Saccharomyces cerevisiae*. *Cell. Mol. Life Sci. 56*, 825−842.

(8) Fischer, H., and Glockshuber, R. (1993) Atp Hydrolysis Is Not Stoichiometrically Linked with Proteolysis in the Atp-Dependent Protease La from Escherichia-Coli. *J. Biol. Chem. 268*, 22502−22507.

(9) Park, S. C., Jia, B., Yang, J. K., Van, D. L., Shao, Y. G., Han, S. W., Jeon, Y. J., Chung, C. H., and Cheong, G. W. (2006) Oligomeric structure of the ATP-dependent protease La (Lon) of Escherichia coli. *Mol. Cells 21*, 129−134.

(10) Rudyak, S. G., Brenowitz, M., and Shrader, T. E. (2001) Mg2+-linked oligomerization modulates the catalytic activity of the Lon (La) protease from Mycobacterium smegmatis. *Biochemistry 40*, 9317−9323.

(11) Patterson, J., Vineyard, D., Thomas-Wohlever, J., Behshad, R., Burke, M., and Lee, I. (2004) Correlation of an adenine-specific conformational change with the ATP-dependent peptidase activity of Escherichia coli Lon. *Biochemistry 43*, 7432−7442.

(12) Vasilyeva, O. V., Kolygo, K. B., Leonova, Y. F., Potapenko, N. A., and Ovchinnikova, T. V. (2002) Domain structure and ATP-induced conformational changes in *Escherichia coli* protease Lon revealed by limited proteolysis and autolysis. *FEBS Lett. 526*, 66−70.

(13) Rotanova, T. V., Melnikov, E. E., Khalatova, A. G., Makhovskaya, O. V., Botos, I., Wlodawer, A., and Gustchina, A. (2004) Classification of ATP-dependent proteases Lon and comparison of the active sites of their proteolytic domains. *Eur. J. Biochem. 271*, 4865−4871.

(14) Amerik, A. Y., Antonov, V. K., Gorbalenya, A. E., Kotova, S. A., Rotanova, T. V., and Shimbarevich, E. V. (1991) Site-directed mutagenensis of La protease: a catalytically active serine protease. *FEBS Lett. 287*, 211−214.

(15) Starkova, N. N., Koroleva, E. P., Rumsh, L. D., Ginodman, L. M., and Rotanova, T. V. (1998) Mutations in the proteolytic domain of Escherichia coli protease Lon impair the ATPase activity of the enzyme. *FEBS Lett. 422*, 218−220.

(16) Fisher, H., and Glockshuber, R. (1993) ATP hydrolysis is not stoichiometrically linked to proteolysis in the ATP-dependent protease La from *Escherichia coli*. *J. Biol. Chem. 268*, 22502−22507.

(17) Fischer, H., and Glockshuber, R. (1994) A Point Mutation within the Atp-Binding Site Inactivates Both Catalytic Functions of the Atp-Dependent Protease La (Lon) from Escherichia-Coli. *FEBS Lett. 356*, 101−103.

(18) Lee, C., Schwartz, M. P., Prakash, S., Iwakura, M., and Matouschek, A. (2001) ATP-dependent proteases degrade their substrates by processively unraveling them from the degradation signal. *Mol. Cell 7*, 627−637.

(19) Nishii, W., Suzuki, T., Nakada, M., Kim, Y. T., Muramatsu, T., and Takahashi, K. (2005) Cleavage mechanism of ATP-dependent Lon protease toward ribosomal S2 protein. *FEBS Lett. 579*, 6846−6850.

(20) Thompson, M. W., Singh, S. K., and Maurizi, M. R. (1994) Processive degradation of proteins by the ATP-dependent Clp protease from Escherichia coli. Requirement for the multiple array of active sites in ClpP but not ATP hydrolysis. *J. Biol. Chem. 269*, 18209−18215.

(21) Kenniston, J. A., Baker, T. A., Fernandez, J. M., and Sauer, R. T. (2003) Linkage between ATP consumption and mechanical unfolding during the protein processing reactions of an AAA+ degradation machine. *Cell 114*, 511−520.

(22) Wang, J., Song, J. J., Franklin, M. C., Kamtekar, S., Im, Y. J., Rho, S. H., Seong, I. S., Lee, C. S., Chung, C. H., and Eom, S. H. (2001) Crystal structures of the HslVU peptidase-ATPase complex reveal an ATP-dependent proteolysis mechanism. *Structure 9*, 177−184.

(23) Goldberg, A. L., Moerschell, R. P., Chung, C. H., and Maurizi, M. R. (1994) ATP-dependent protease La (Lon) from *Escherichia coli*. *Meth. Enzymol. 244*, 350−375.

(24) Reid, B. G., Fenton, W. A., Horwich, A. L., and Weber-Ban, E. U. (2001) ClpA mediates directional translocation of substrate proteins into the ClpP protease. *Proc. Natl. Acad. Sci. U. S. A. 98*, 3768−3772.
(25) Maurizi, M. R. (1987) Degradation in vitro of bacteriophage lambda N protein by Lon protease from Escherichia coli. *J. Biol. Chem. 262*, 2696−2703.
(26) Ondrovicova, G., Liu, T., Singh, K., Tian, B., Li, H., Gakh, O., Perecko, D., Janata, J., Granot, Z., Orly, J., Kutejova, E., and Suzuki, C. K. (2005) Cleavage site selection within a folded substrate by the ATP-dependent lon protease. *J. Biol. Chem. 280*, 25103−25110.
(27) Kandror, O., Sherman, M., and Goldberg, A. (1999) Rapid degradation of an abnormal protein in Escherichia coli proceeds through repeated cycles of association with GroEL. *J. Biol. Chem. 274*, 37743−37749.
(28) Licht, S., and Lee, I. (2008) Resolving individual steps in the operation of ATP-dependent proteolytic molecular machines: from conformational changes to substrate translocation and processivity. *Biochemistry 47*, 3595−3605.
(29) Farbman, M. E., Gershenson, A., and Licht, S. (2008) Role of a conserved pore residue in the formation of a prehydrolytic high substrate affinity state in the AAA+ chaperone ClpA. *Biochemistry 47*, 13497−13505.
(30) Kolygo, K., Ranjan, N., Kress, W., Striebel, F., Hollenstein, K., Neelsen, K., Steiner, M., Summer, H., and Weber-Ban, E. (2009) Studying chaperone-proteases using a real-time approach based on FRET. *J. Struct. Biol. 168*, 267−277.
(31) Rajendar, B., and Lucius, A. L. (2010) Molecular mechanism of polypeptide translocation catalyzed by the Escherichia coli ClpA protein translocase. *J. Mol. Biol. 399*, 665−679.
(32) Gottesman, S., Roche, E., Zhou, Y. N., and Sauer, R. T. (1998) The ClpXP and ClpAP proteases degrade proteins with carboxy-terminal peptide tails added by the SsrA-tagging system. *Genes Dev. 12*, 1338−1347.
(33) Martin, A., Baker, T. A., and Sauer, R. T. (2008) Pore loops of the AAA plus ClpX machine grip substrates to drive translocation and unfolding. *Nat. Struct. Mol. Biol. 15*, 1147−1151.
(34) Rees, W. A., Weitzel, S. E., Yager, T. D., Das, A., and von Hippel, P. H. (1996) Bacteriophage lambda N protein alone can induce transcription antitermination in vitro. *Proc. Natl. Acad. Sci. U. S. A. 93*, 342−346.
(35) Mogridge, J., Legault, P., Li, J., Van Oene, M. D., Kay, L. E., and Greenblatt, J. (1998) Independent ligand-induced folding of the RNA-binding domain and two functionally distinct antitermination regions in the phage lambda N protein. *Mol. Cell 1*, 265−275.
(36) Legault, P., Li, J., Mogridge, J., Kay, L. E., and Greenblatt, J. (1998) NMR structure of the bacteriophage lambda N peptide/boxB RNA complex: recognition of a GNRA fold by an arginine-rich motif. *Cell 93*, 289−299.
(37) Van Gilst, M. R., Rees, W. A., Das, A., and von Hippel, P. H. (1997) Complexes of N antitermination protein of phage lambda with specific and nonspecific RNA target sites on the nascent transcript. *Biochemistry 36*, 1514−1524.
(38) Prasch, S., Schwarz, S., Eisenmann, A., Wohrl, B. M., Schweimer, K., and Rosch, P. (2006) Interaction of the intrinsically unstructured phage lambda N Protein with Escherichia coli NusA. *Biochemistry 45*, 4542−4549.
(39) Lee, I., and Berdis, A. J. (2001) Adenosine triphosphate-dependent degradation of a fluorescent lambda N substrate mimic by Lon protease. *Anal. Biochem. 291*, 74−83.
(40) Patterson-Ward, J., Tedesco, J., Hudak, J., Fishovitz, J., Becker, J., Frase, H., McNamara, K., and Lee, I. (2009) Utilization of synthetic peptides to evaluate the importance of substrate interaction at the proteolytic site of Escherichia coli Lon protease. *Biochim. Biophys. Acta 1794*, 1355−1363.
(41) Bradford, M. M. (1976) A rapid and sensitive method for the quantitation of microgram quantities of protein utilizing the principle of protein-dye binding. *Anal. Biochem. 72*, 248−254.
(42) Cheng, I., Mikita, N., Fishovitz, J., Frase, H., Wintrode, P., and Lee, I. (2012) Identification of a region in the N-terminus of Escherichia coli Lon that affects ATPase, substrate translocation and proteolytic activity. *J. Mol. Biol. 418*, 208−225.
(43) Thomas-Wohlever, J., and Lee, I. (2002) Kinetic characterization of the peptidase activity of Escherichia coli Lon reveals the mechanistic similarities in ATP-dependent hydrolysis of peptide and protein substrates. *Biochemistry 41*, 9418−9425.
(44) Liu, T., D'Mello, V., Deng, L., Hu, J., Ricardo, M., Pan, S., Lu, X., Wadsworth, S., Siekierka, J., Birge, R., and Li, H. (2006) A multiplexed proteomics approach to differentiate neurite outgrowth patterns. *J. Neurosci. Methods 158*, 22−29.
(45) Lakowicz, J. R. (1999) *Principles of fluorescence spectroscopy*, Kluwer Academic/Plenum Publishers, New York.
(46) Gutfreund, H. (1995) *Kinetics for Life Sciences*, Cambridge University Press, United Kingdom.
(47) Patterson-Ward, J., Huang, J., and Lee, I. (2007) Detection and characterization of two ATP-dependent conformational changes in proteolytically inactive Escherichia coli lon mutants by stopped flow kinetic techniques. *Biochemistry 46*, 13593−13605.
(48) Ortega, J., Singh, S. K., Ishikawa, T., Maurizi, M. R., and Steven, A. C. (2000) Visualization of substrate binding and translocation by the ATP-dependent protease, ClpXP. *Mol. Cell 6*, 1515−1521.
(49) Kenniston, J. A., Burton, R. E., Siddiqui, S. M., Baker, T. A., and Sauer, R. T. (2004) Effects of local protein stability and the geometric position of the substrate degradation tag on the efficiency of ClpXP denaturation and degradation. *J. Struct. Biol. 146*, 130−140.
(50) Stryer, L. (1959) Intramolecular resonance transfer of energy in proteins. *Biochim. Biophys. Acta 35*, 242−244.
(51) Cha, S. S., An, Y. J., Lee, C. R., Lee, H. S., Kim, Y. G., Kim, S. J., Kwon, K. K., De Donatis, G. M., Lee, J. H., Maurizi, M. R., and Kang, S. G. (2010) Crystal structure of Lon protease: molecular architecture of gated entry to a sequestered degradation chamber. *EMBO J. 29*, 3520−3530.
(52) Vineyard, D., Patterson-Ward, J., Berdis, A. J., and Lee, I. (2005) Monitoring the timing of ATP hydrolysis with activation of peptide cleavage in Escherichia coli Lon by transient kinetics. *Biochemistry 44*, 1671−1682.
(53) Gur, E., and Sauer, R. T. (2008) Recognition of misfolded proteins by Lon, a AAA(+) protease. *Genes Dev. 22*, 2267−2277.
(54) Venkatesh, S., Lee, J., Singh, K., Lee, I., and Suzuki, C. K. (2012) Multitasking in the mitochondrion by the ATP-dependent Lon protease. *Biochim. Biophys. Acta 1823*, 56−66.
(55) Choi, K. H., and Licht, S. (2005) Control of peptide product sizes by the energy-dependent protease ClpAP. *Biochemistry 44*, 13921−13931.